THESIS FOR THE DEGREE OF DOCTOR OF PHILOSOPHY

Pushing methods for plasma simulations into the QED regime

Erik Wallin

Department of Physics
CHALMERS UNIVERSITY OF TECHNOLOGY

Gothenburg, Sweden 2018

Pushing methods for plasma simulations into the QED regime
Erik Wallin
ISBN 978-91-7597-778-2

Doktorsavhandlingar vid Chalmers tekniska högskola
Ny serie nr 4459
ISSN 0346-718X

Department of Physics
Chalmers University of Technology
SE-412 96 Gothenburg
Sweden
Telephone: +46 (0)31-772 1000

Cover:
"Artist"'s rendition of electrons accelerated behind a short, intense laser pulse in laser wakefield acceleration.

Chalmers Reproservice
Gothenburg, Sweden 2018

Pushing methods for plasma simulations into the QED regime
ERIK WALLIN
Department of Physics
Chalmers University of Technology

Abstract

The interaction between a super-intense laser pulse, with intensity up to $10^{22}\mathrm{W/cm}^2$, and a plasma opens new regimes of physics, with new questions and more demand on existing numerical tools. Relativistic and quantum effects which are negligible for lower laser intensities become important and must be properly modelled to generate reliable predictions. Increased laser intensity opens up previously unexplored or unattainable regimes and allows for the study of basic physical phenomenon, such as when energy loss through radiation starts to have large effects on particle dynamics.

In this thesis we develop schemes to include high intensity radiation from relativistic particles in classical particle-in-cell plasma simulations, with the corresponding energy loss from classical electrodynamics as well as quantum electrodynamic theory. We examine the effect of properly modelling radiation energy losses for laser wakefield acceleration. We propose a novel, tunable scheme for generation of X-ray radiation through interacting laser wakefields, while also finding a regime with strong and stable electron bunch oscillations. We examine the difference between classical and quantum theory in the collision between a laser pulse and an electron, proposing experimental signatures for detection of effects of quantum radiation reaction, a stochastic effect of energy loss through radiation. Furthermore, we use the *Manley-Rowe relations* to verify the form of a term in the equations for quantum hydrodynamics.

KEYWORDS: plasma, nonlinear dynamics, Manley-Rowe, particle-in-cell, synchrotron radiation, radiation reaction, LWFA

Publications

This thesis is based on the following publications:

1. **Three-wave interaction and Manley-Rowe relations in quantum hydrodynamics**
   E. Wallin, J. Zamanian, G. Brodin
   J. Plasma Phys. **80** 643 (2014).

2. **Narrowing of the emission angle in high-intensity Compton scattering**
   C.N. Harvey, A. Gonoskov, M. Marklund, E. Wallin
   Phys. Rev. A **93**, 022112 (2016).

3. **Effects of high energy photon emissions in laser generated ultra-relativistic plasmas: Real-time synchrotron simulations**
   E. Wallin, A. Gonoskov, M. Marklund
   Phys. Plasmas **22**, 033117 (2015).

4. **Extended particle-in-cell schemes for physics in ultrastrong laser fields: Review and developments**
   A. Gonoskov, S. Bastrakov, E. Efimenko, A. Ilderton, M. Marklund, I. Meyerov, A. Muraviev, A. Sergeev, I. Surmin, E. Wallin
   Phys. Rev. E **92**, 023305 (2015).

5. **Radiation emission from braided electrons in interacting wakefields**
   E. Wallin, A. Gonoskov, M. Marklund
   Phys. Plasmas **24**, 093101 (2017).

6. **Ultra-intense laser pulses in near-critical underdense plasmas - radiation reaction and energy partitioning**
   E. Wallin, A. Gonoskov, C. Harvey, O. Lundh, M. Marklund
   J. Plasma Phys. **83** 2 (2017).

Other publications by the author that are not included in the thesis:

- **Scalar Wigner theory for polarized light in nonlinear Kerr media**
  T. Hansson, E. Wallin, G. Brodin, M. Marklund
  J. Opt. Soc. Am. B **30**, 1765 (2013).

Contents

Chapter 1

Introduction

An important part of physics is concerned with making models. Given some experimental results, we try to develop models which can reproduce and explain the given results as well as predict new phenomena. Experiments of such phenomena can then be attempted and the theory can be strengthened or could turn out to be invalid in some new regime, prompting the need for a new theory. In such a way we can get a hierarchy of models. Some might be simple to apply but are only valid in certain situations. Some might be very hard to apply, but are needed in extreme conditions. The underlying physics is the same, but for some cases we can apply a simplified model. This thesis will present such situations.

Some experiments in physics can be hard to interpret. The reasons can differ, but one such example is if the duration is extremely short, say below 10^{-12} s. The input is known and one can analyse the output, but what happens in between? This can be answered by simulations. By constructing a computer model, including the required physics, one can see what happens during this short, often very complex, interaction. The more complex interaction, the more requirements on the simulations to include appropriate physics.

In this thesis we consider the interaction between waves (e.g. a laser) and a plasma, studying extensions of well-known plasma theory and of plasma simulation methods to account for physics in different regimes. This includes relativistic and quantum effects, which we consider from different perspectives.

From a theoretical perspective we consider extensions to plasma fluid equations to account for quantum effects, described in quantum hydrodynamics. This accounts for quantum effects in low temperature, high density plasmas related e.g. to the fact that fermions cannot occupy the same energy states.

We also consider extensions to numerical methods for laser-plasma interactions to enable simulations of high intensity lasers where relativistic

and quantum effects must be handled. These are different types of quantum effects, when the emission of single photons have high enough energy so that they significantly affect the motion of the emitting particle. In more extreme cases photons may contain more energy than the rest mass of an electron and a positron together and can go on to produce such a pair of particles.

One important application of laser-plasma interaction is the generation of high energy particles, a *plasma accelerator* with potential to compete with conventional accelerators, especially regarding the important factor of size. Since allowing much stronger fields, a plasma accelerator has the potential to accelerate particles in much shorter distances and can thus be made much smaller.

1.1 Particle accelerators

Highly energetic particles can be of great use, with applications in medicine (diagnosis and treatment) [1, 2], biology, industry (non-destructive detection) and physics e.g.[3, 4] However, accelerating particles to close to the speed of light is no easy experimental task. Conventional types of accelerators accelerate particles through strong fields in either a straight line (linear accelerator), a spiral (cyclotron) or in a circle (synchrotron), with different advantages and disadvantages. In a linear accelerator the energy loss through radiation is very small, a cyclotron can provide a continuous flow of particles and in a synchrotron the field strength of the magnets turning the particles are synchronized with the particle energies to produce a closed loop, reusing the accelerating fields to gain energy during many laps. However, one common disadvantage is that these facilities are large; room sized at least for energies of the order of GeV and *huge* (km sized) for higher energies (order of TeV).

For these reasons high energy facilities are expensive and rare, e.g. the 27 km in circumference Large Hadron Collider [5] at CERN at several billion US$ or the 3.2 km long linear accelerator SLAC [6] at hundreds of million US$, and there is no easy way to overcome the required size. The strength of the accelerating fields are typically operated at $\sim$ 10MV/m, and could maximally be $\sim$ 100MV/m, in order to not ionize the accelerator walls (field emission) and due to the theoretical breakdown of superconductors. The field emission may be limited, but the theoretical breakdown of superconductors may not. In order to e.g. achieve 1 GeV electrons this gives acceleration distances of the order of $\sim$ 100 m. The linear accelerator must for obvious reasons be very long as the particle only make a single pass, but even reusing the accelerating fields as in a synchrotron does not provide a solution.

For heavy particles the field strength will be a limiting factor in turning the particles in a circle. This can be a problem for ions, but also light

particles such as electrons can turn heavy as their effective mass increase with energy, with e.g. 1 GeV electrons being ~ 2000 times as massive as in rest. Furthermore, the lighter the particle and the smaller the radius of the circular motion, the more of its energy it will lose through radiation. The energy loss will eventually balance the energy gain and limit the achievable energy if the circle is not big enough.

1.2 Plasma accelerators

Plasma accelerators can provide an alternative to conventional accelerators. Here particles are accelerated in the interaction between a *super-intense*, *ultra-short* laser pulse and a plasma, created when the so called pre-pulse of the laser interact with a target (e.g. a gas or a metal foil). With fields strengths up to ~ 100 GV/m [7–11], a factor more than 1000 increase from conventional accelerators, the particles can be accelerated in very short distances, e.g. ~ 1 GeV electrons accelerated in ~ 1 cm in laser wakefield acceleration (LWFA) [12]. This can result in smaller, less expensive facilities as well as unique applications, e.g. with ultra-short ($\sim 10^{-15}$s) bursts of X-rays.

The intensity of short pulse lasers has seen a steady rise since the invention of chirped pulse amplification [13] in the 1980s. Present state-of-the-art laser systems can focus $\sim$10 J of energy to a target of a few μm in $\sim$10 fs, (e.g. Hercules [14]) approaching intensities of 10^{22} W/cm^2 with capacity of accelerating particles to very high energies on a centimeter scale, as e.g. GeV electrons in LWFA or MeV ions in target normal sheath acceleration [15–17]. Coming facilities[18] will provide even more energy, taking the maximum intensity towards $\sim 10^{23}$ W/cm^2.

The main theme in this thesis is *laser-matter interaction*. We focus on these so called super-intense, ultra short laser pulses. Their duration are very short, measured in tens of femtoseconds (fs $= 10^{-15}$ s). However, during this short time, the intensity of the radiation is comparable to taking all the light from the sun hitting the earth and focus this down to ~ 1 cm^2. When such a laser pulse interacts with matter, be it a gas or a metal, the electromagnetic fields of the laser surpass the electrostatic fields from the atomic nucleus keeping the electrons in place. The motion of the electrons is then governed by the laser pulse and not by the nucleus. The atoms are ionized, forming a *plasma*.

Many of the effects in laser-plasma interactions are highly nonlinear and difficult to analyse analytically. For such problems, computer simulations are a great tool. These may be of different types, e.g. Vlasov codes and particle-in-cell (PIC) codes. The PIC method [19, 20] has become a standard method for simulations of laser-plasma interaction. Here the plasma is modelled as an ensemble of particles moving in an electromagnetic field defined on a

grid. For each iteration the charge- and current densities are weighted to the grid. These are then used to solve the updated fields, the forces from these fields are weighted back to the particles, which propagate according to their equation of motion, and the process is repeated.

In this thesis we consider extensions to numerical methods to handle all the physics involved in these highly nonlinear, ultra relativistic interactions. We explore the fundamental question of particles loosing energy through radiation and propose a novel, tunable scheme for X-ray generation from accelerated electrons.

1.3 Outline

We begin by considering the properties of a *plasma*. This everyday exotic, but on a universal scale extremely common, state of matter is of central importance and will be described in detail in Chapter 2. Sections 2.1 - 2.3 describe plasma properties, plasma equations and plasma waves. Sections 2.4 - 2.5 are introductions to wave-wave interaction covered in Paper I and are not required for understanding the rest of the thesis.

A plasma can be seen as a gas of charged particles, typically electrons and ions. However, as unlike a gas the particles have an electric charge and their motion constitute a current, the description of a plasma is not possible without the description of electric and magnetic fields. Maxwell's equations for electromagnetic fields are presented in Section 2.2, and Chapter 3 focus on how the motion of single charges produce electromagnetic radiation. Here we also face the breakdown of classical electromagnetic theory, where trying to include the energy loss due to radiation for the radiating particle prove to be too much of a problem. This energy loss due to radiation, termed the *radiation reaction*, is described in Section 3.2 with a classical approximation presented, valid as long as the energy loss is small compared to the kinetic energy of the particle. Radiation and radiation reaction are central themes in the thesis, and are discussed in papers II-VI.

In Section 3.3 quantum electromagnetic theory in relation to radiation reaction is discussed. This provides solutions when classical theory breaks down: describing evolution of high energy particles interacting with strong electromagnetic fields, where the emitted radiation is comparable to the kinetic energy of the emitting particles. This is an introduction to Paper II, where this is covered.

In Chapter 4, the *particle-in-cell* method is presented. This is a common method for plasma computer simulations, in which the electric and magnetic fields are solved on a grid with plasma particles moving within. The classical particle-in-cell scheme is presented in Section 4.1. In Section 4.2 extensions to this scheme in order to handle high energy radiation and radiation reaction described above, are discussed. This connects directly to papers III

and IV, where such extensions are presented and analysed and indirectly to papers V and VI where they are applied to analyse new physics.

Chapter 5 gives an introduction to *laser wakefield acceleration*, which is a method for electron acceleration where electrons are accelerated to relativistic energies in the wakefield of a laser propagating through a plasma.

Finally, Chapter 6 focus on radiation from laser wakefields. This is an introduction to Paper V where we propose a new scheme for radiation generation through colliding wakefields, and Paper VI where we examine the effect of radiation reaction on the laser wakefield acceleration scheme.

The papers covered in this thesis adopt different systems of units: SI, Gaussian CGS and natural units; all depending on the convention in their respective subfield. In this thesis we adopt Gaussian CGS units in general, except in section 2.5 covering details of Paper I where SI units are used.

Chapter 2

Plasma

A plasma is a complicated state of matter. Unlike a common gas, the particles in the plasma carry an electric charge. This means they can interact through the electric and magnetic fields that they generate, which allows for complex collective behaviour. Whereas waves in a gas, i.e. sound, propagates through simple collisions between the particles; there is a multitude of different waves in a plasma with different coupling between particle motion and fields depending on wave frequencies and field directions for example. In this chapter we will cover how plasma particle moves to cancel each other's electric fields and the important concept of plasma oscillations, which turn up in many plasma waves. Finally, we look at nonlinear theory, with a focus on wave-wave interaction.

2.1 Plasma properties

A plasma is an ionized gas. Most plasmas are weakly coupled, such that the kinetic energy of a particle is greater than the potential energy due to the nearest neighbour [21]. Heating a gas, gradually the electrons will separate from the atoms to form a gas of electrons and ions, i.e. a plasma.

One important plasma concept is that of *Debye shielding* [22, 23]. If one introduce a test charge q_T in a plasma of density n and temperature T the surrounding particles will be affected by the field from the test charge and will move to try to cancel this field. This is more efficient the denser and colder the plasma is, and the effect is that the test charge is effectively shielded a few distances λ_D away where λ_D, termed the *Debye length*, is given by

$$\lambda_D = \sqrt{\frac{kT}{4\pi n e^2}} \tag{2.1}$$

in CGS-units, where k is Boltzmann's constant and $-e$ the charge of the electron. In Fig. 2.1 the electric potential for a free charged particle and the effect of Debye shielding on a charged particle in a plasma can be seen,

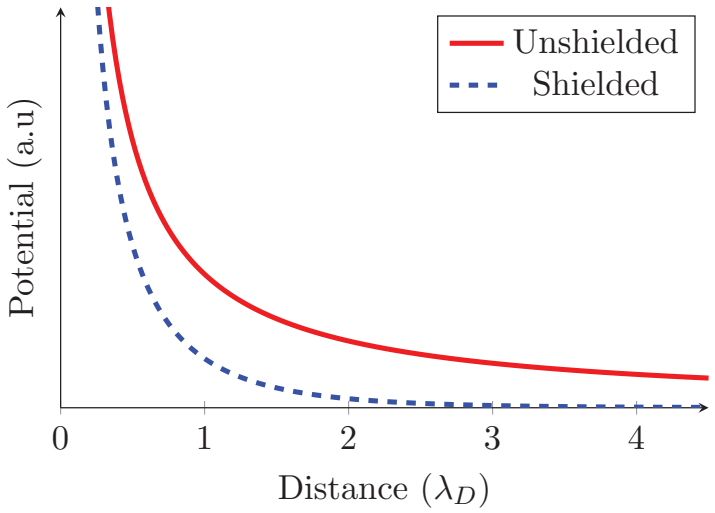

Figure 2.1: The electric potential of a point charge with and without Debye shielding.

where there is an additional exponential drop such that particles a distance $r \gg \lambda_D$ away from the test charge are effectively shielded from its field. It turns out that another way to define a plasma is to demand that a cube with the sides of the Debye length should contain many particles, $n\lambda_D^3 \gg 1$ (if this was not true then there would be very few particles there to do the shielding). This is equivalent to demanding that the typical kinetic energy of the particles should be larger than the typical potential energy due to the nearest neighbour [21].

The fact that the particles in a plasma can generate, and respond to, electromagnetic (EM) fields enables it to support many types of waves, especially if one apply an external magnetic field. If we consider an ion-electron plasma the ions are much heavier than the electrons, with e.g. the proton being $\sim$ 2000 times heavier than the electron. This makes the electrons much more mobile and unless the considered waves are of low frequency, the ions will not have time to move and can be regarded as a neutralizing background with all the density perturbations due to the electrons. If one introduce a density perturbation for the electrons in an otherwise neutral plasma, the charge separation will give rise to an electric field. This will force the electrons back towards their original position, but due to their velocity they will overshoot in the other direction, creating *plasma oscillations*, oscillating with a frequency given by the *plasma frequency*

$$\omega_p = \sqrt{\frac{4\pi n_e e^2}{m_e}} \tag{2.2}$$

where n_e and m_e are the electron density and mass. If the plasma has a nonzero temperature T, these oscillations can propagate in the form of *Langmuir waves*. This can be described by the *dispersion relation*, giving

the relation between the frequency ω and wave number k of the wave. For a Langmuir wave the dispersion relation is

$$\omega^2 = \omega_p^2 + 3k^2 v_e^2, \tag{2.3}$$

valid for $v_e \ll \omega_p/k$, where $v_e = \sqrt{k_B T/m}$ is the thermal velocity of the electrons. From the dispersion relation one can deduce several important properties of the wave, e.g. group velocity (the speed of a wave envelope) and dispersion (the spreading of a wave envelope).

Another type of wave in a plasma is the *electromagnetic plasma wave*. Similarly to the case of propagation in vacuum, this is a wave with a transverse E- and B-field, with the difference from waves in vacuum being that the speed of the wave is affected by the plasma. Here the dispersion relation is given by

$$\omega^2 = \omega_p^2 + k^2 c^2 \tag{2.4}$$

where c is the speed of light and ω_p is the plasma frequency defined in Eq. (2.2). The case of an electromagnetic wave in vacuum can be retrieved by letting the plasma density approach zero, such that $\omega_p \to 0$ with the dispersion relation reducing to $\omega^2 = k^2 c^2$.

For an electromagnetic wave with frequency ω travelling in vacuum and entering a plasma, the possibility of propagation in the plasma depends on the plasma frequency. If $\omega < \omega_p$ then there are no real solutions for k in Eq. (2.4) and the wave can not propagate in the plasma, but will instead be exponentially damped inside the plasma and will be reflected. On the other hand, $\omega > \omega_p$ gives real valued solutions of k and the electromagnetic wave can propagate in the plasma. Thus, depending on the plasma frequency (and hence directly on the density) the plasma can either be transparent or opaque for EM radiation. For a laser with frequency ω the *critical density* is given by

$$n_{\text{crit}} = \frac{m_e \omega^2}{4\pi e^2} \tag{2.5}$$

where for densities $n \leq n_{\text{crit}}$ the plasma is *underdense* and transparent in the absence of collisions, and for densities $n \geq n_{\text{crit}}$ the plasma is *overdense* and opaque.

2.2 Plasma descriptions

The two main ways of modelling a plasma are the *kinetic* and *fluid* plasma descriptions.

2.2.1 Kinetic description

In kinetic theory the plasma is described by the distribution functions $f_s(\mathbf{r}, \mathbf{v}, t)$ representing the number of particles of species s, (usually $s = e, i$ for elec-

trons and ions) at position $\mathbf{r}$ with velocity $\mathbf{v}$, at time t. The evolution of this system in time is then given by the *Vlasov equation* [24]

$$\frac{\partial f_s(\mathbf{r},\mathbf{v},t)}{\partial t} + \mathbf{v}\cdot\frac{\partial f_s(\mathbf{r},\mathbf{v},t)}{\partial \mathbf{r}} + \frac{q_s}{m_s}\left(\mathbf{E}+\frac{\mathbf{v}}{c}\times\mathbf{B}\right)\cdot\frac{\partial f_s(\mathbf{r},\mathbf{v},t)}{\partial \mathbf{v}} = 0, \quad (2.6)$$

together with Maxwell's equations

$$\nabla\cdot\mathbf{E} = 4\pi\rho \quad (2.7)$$

$$\nabla\cdot\mathbf{B} = 0 \quad (2.8)$$

$$\nabla\times\mathbf{E} = -\frac{1}{c}\frac{\partial\mathbf{B}}{\partial t} \quad (2.9)$$

$$\nabla\times\mathbf{B} = \frac{4\pi}{c}\mathbf{J} + \frac{1}{c}\frac{\partial\mathbf{E}}{\partial t} \quad (2.10)$$

for the fields, where $\mathbf{E}$ is the electric field, $\mathbf{B}$ is the magnetic field, ρ is the charge density and $\mathbf{J}$ is the current density. The latter two are given in terms of the distribution functions by

$$\rho(\mathbf{r}) = \sum_s q_s \int f_s(\mathbf{r},\mathbf{v},t)\mathrm{d}^3v \quad (2.11)$$

and

$$\mathbf{J}(\mathbf{r}) = \sum_s q_s \int \mathbf{v} f_s(\mathbf{r},\mathbf{v},t)\mathrm{d}^3v \quad (2.12)$$

respectively. Fig. 2.2 shows a simplified example of a distribution function, evolving from time t_0 to t_1 through the Vlasov equation. The Vlasov equation is probably the most important plasma equation and can describe a large variety of plasma phenomenon. Still, it does not take collisions into account. However, for a weakly coupled plasma where $n\lambda_D^3 \gg 1$, the collisional effects are small compared to the collective plasma effects [23].

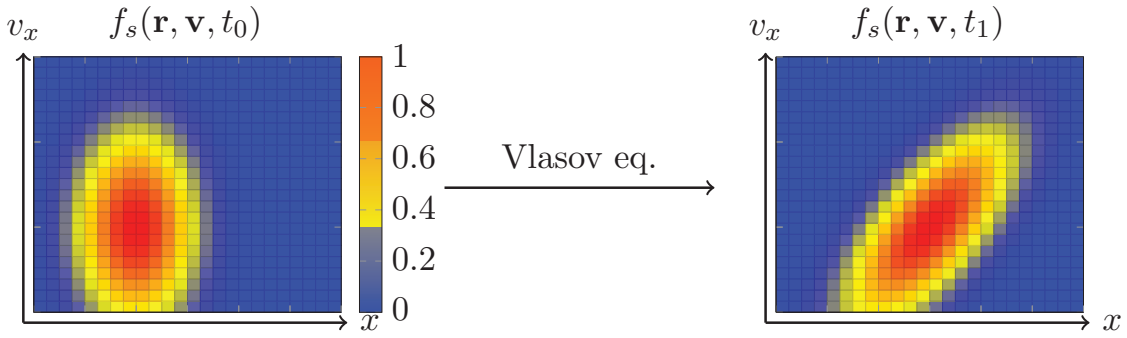

Figure 2.2: Illustration of a distribution function $f_s(\mathbf{r},\mathbf{v},t)$, evolved in time through the Vlasov equation.

2.2.2 Fluid description

The fluid description is a simplification of the Vlasov equation, where each species of the plasma is considered as interpenetrating fluids. The equations are derived by taking velocity moments of the Vlasov equation. In principle the result is an infinite series of equations of three dimensions, replacing the six-dimensional Vlasov equation. In practice though, the series is truncated using physical arguments to give a limited amount of equations, typically two or three. Integrating the Vlasov equation over all velocities results in the *continuity equation*,

$$\frac{\partial n_s}{\partial t} + \nabla \cdot (n_s \mathbf{v}_s) = 0 \tag{2.13}$$

with $n_s = n_{e,i}(\mathbf{r})$ and $\mathbf{v}_s = \mathbf{v}_{e,i}(\mathbf{r})$ representing the number density and mean velocity of the electrons and ions respectively. The continuity equation describes the fact that the fluid is not created nor destroyed. Multiplying the Vlasov equation by $\mathbf{v}$ and integrating over all velocities results in the *momentum equation*

$$\frac{\partial \mathbf{v}_s}{\partial t} + (\mathbf{v}_s \cdot \nabla)\, \mathbf{v}_s = -\frac{\nabla P}{n_s m_s} + \frac{q_s}{m_s}\big(\mathbf{E} + \frac{\mathbf{v}_s}{c} \times \mathbf{B}\big) \tag{2.14}$$

describing the effect of forces on the fluid. Here P is the pressure and to have a complete description we need to have a pressure model in which P is expressed in terms of known quantities, where a common model is $Pn^{-\gamma} = \text{const}$. Fluid theory is a rather crude approximation of kinetic theory. As such there are situations where it is easier to work with and where it gives the same result as kinetic theory. However, the dependence of the velocity distribution is lost and effects where this is of importance can not be calculated using fluid theory, e.g. *Landau damping* [25]. Fig. 2.3 illustrates how the velocity dependence of the distribution function $f_s(\mathbf{r}, \mathbf{v}, t)$ is integrated away to get a density function. Considering plasma in a small region in space, this is now described by a density and a single fluid velocity according to $n_{e,i}(\mathbf{r})$ and $\mathbf{v}_{e,i}(\mathbf{r})$, instead of a distribution of velocities according to $f_{e,i}(\mathbf{r}, \mathbf{v}, t)$.

2.3 Linear theory and plasma waves

As mentioned above, a plasma supports a multitude of waves. In order to find these wave solutions we *linearize* the plasma equations; considering small perturbations of the involved parameters, with e.g. the density written as the sum of two components

$$n = n_0 + n_1(\mathbf{r}, t) \tag{2.15}$$

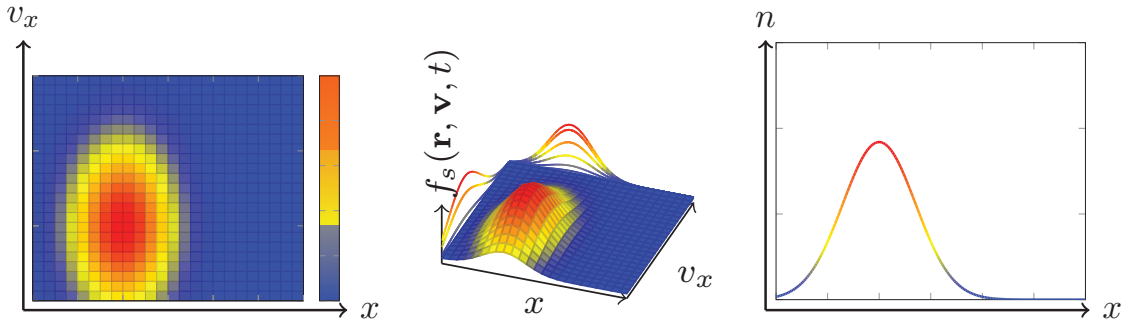

Figure 2.3: Illustration of how the velocity dependence of the distribution function $f_s(\mathbf{r}, \mathbf{v}, t)$ is integrated away to give a density function. $f_s(\mathbf{r}, \mathbf{v}, t)$, shown on the left and in the middle, depend on both position and velocity so in each position there is a distribution of velocities, whereas for the fluid description the plasma at a certain position $\mathbf{r}$ has a single value for the velocity. The density, $n(\mathbf{r})$ can be seen on the right, or in the marginal distribution in the middle.

where n_0 is the unperturbed, constant background value and $n_1 \ll n_0$ being a time- and space dependent perturbation. Depending on the considered situation, these assumptions will be different and will result in different wave solutions. We can e.g. consider cases where there is no background magnetic field or where the background magnetic field is along some direction, resulting in different wave solutions representing different types of possible plasma waves.

In linear theory we consider the perturbations so small so the product of two perturbations, e.g. $n_1 E_1$, is negligible compared to a single perturbation term, e.g. n_1. Thus, we only consider results up to first order in the small perturbations. The result is a system of equations for the involved perturbations and background values, where wave solutions can be found by looking for solutions of the form

$$n_1(\mathbf{r}, t) = \tilde{n}_1 \exp(-i\omega t + i\mathbf{k} \cdot \mathbf{r}) \tag{2.16}$$

where $\tilde{n}_1$ is the amplitude, $\mathbf{k}$ the wave vector and ω the frequency. The complex expression is used for convenience. As the equations are linear, the physical solution can be retrieved by taking the real part in the end. The result is a relation between the frequency ω and the wave vector $\mathbf{k}$, i.e. a dispersion relation, mentioned in Section 2.1. This procedure, with appropriate linearization, allow us to derive dispersion relations for a large number of plasma waves (e.g. Langmuir waves, ion-acoustic waves and electromagnetic waves). A simple example is if we neglect ion motion, put $T = 0$ and linearize according to $n_e = n_0 + n_1(\mathbf{r}, t)$, $E = E_1(\mathbf{r}, t)$ and $v_e = v_1(\mathbf{r}, t)$ we can derive the plasma oscillations $\omega = \pm\omega_p$ mentioned above. For further reading on this, see e.g. [23].

2.4 Nonlinear theory and wave-wave interaction

In nonlinear theory we consider larger perturbations, where the product of two perturbations can no longer be neglected, as they were in linear theory. This opens up for several effects not present in linear theory. One such effect is that of wave-wave interaction, where energy is transferred between interacting waves. This is in contrast to linear theory, where the superposition principle applies and energy can not be transferred between waves in a homogeneous medium.

We consider three interacting waves, with e.g. the electric field given by (and similar for the magnetic field, density and velocity)

$$E = E_{(1)}e^{i(k_{(1)}r-\omega_{(1)}t)} + E_{(2)}e^{i(k_{(2)}r-\omega_{(2)}t)} + E_{(3)}e^{i(k_{(3)}r-\omega_{(3)}t)} + \text{c.c.} \quad (2.17)$$

where c.c. denotes the complex conjugate and $E_{(i)}$, $\omega_{(i)}$ and $k_{(i)}$ denotes the amplitude, frequency and wave number of the i:th wave. This ansatz is suitable for weakly nonlinear waves where we can apply perturbation calculations. The time-dependence of the amplitudes is slow compared to the frequency as the interaction is weak. Here we must add the complex conjugate to make the expression real from the start, since the real and imaginary parts are not independent solutions as in linear theory. We also consider the following relation between the frequencies and wave vectors of the three waves,

$$\begin{aligned} \omega_{(3)} &= \omega_{(1)} + \omega_{(2)} \\ \mathbf{k}_{(3)} &= \mathbf{k}_{(1)} + \mathbf{k}_{(2)}, \end{aligned} \quad (2.18)$$

which will be necessary in order to derive equations for the evolution of the wave amplitudes. Classically (2.18) is referred to as frequency and wave vector matching, but it can also be viewed as energy and momentum conservation of individual wave quanta.

Here one could consider the case of having one wave from the start, entering a plasma region. There will be noise in that region, which could be decomposed into different frequencies. Some of these perturbations can match with the incoming wave according to the relations in Eq. (2.18) and those waves can grow, taking energy from the initial wave.

Entering the expression for the fields, densities and velocities on the form of Eq. (2.17) into the plasma fluid equations, there will be a lot of nonlinear terms that are products of parts from the three different waves. For each term in the fluid equations involving a product of two quantities there will be $6^2 = 36$ such nonlinear terms (from the 3 conjugate and 3 non-conjugate terms of each quantity). It turns out that not all of these terms are important when it comes to how the amplitude of each wave will evolve, depending on their timescale. Only terms oscillating with similar frequencies will be of importance, as the other will be out of phase and

over a longer time their average contribution will be 0. In order to simplify this, and get expressions for how the amplitude of each wave (represented as the amplitude of e.g. the electric field) will develop, one can filter out the frequency of that wave. By e.g. multiplying Eq. (2.17) by $e^{-i(k_{(3)}r-\omega_{(3)}t)}$ and taking the average over many periods one will single out the $E_{(3)}$ part, as all other terms will be rapid oscillations giving 0 in average, whereas the $E_{(3)}$ part will be constant. Similarly, using the relations in Eq. (2.18) one can single out contributing nonlinear terms in the fluid equations. E.g. the term matching with $E_{(3)}$ from $\mathbf{v} \times \mathbf{B}$ will be

$$v_{(2)}B_{(1)} \propto e^{i\left((k_{(1)}+k_{(2)})r-(\omega_{(1)}+\omega_{(2)})t\right)} = e^{i(k_{(3)}r-\omega_{(3)}t)}. \tag{2.19}$$

In this manner, we can eventually get equations for how the wave amplitudes will evolve, on the form

$$\frac{\mathrm{d}E_{(3)}}{\mathrm{d}t} = c_3 E_{(1)} E_{(2)} \tag{2.20}$$

$$\frac{\mathrm{d}E_{(2)}}{\mathrm{d}t} = c_2 E_{(3)} E^*_{(1)} \tag{2.21}$$

$$\frac{\mathrm{d}E_{(1)}}{\mathrm{d}t} = c_1 E^*_{(2)} E_{(3)} \tag{2.22}$$

where we have used linear relations to express all the nonlinear terms as the same variable (the electric field in this case). c_i represent the coupling coefficients, describing how the different waves couple to each other.

It turns out that there is a restriction in how the waves can exchange energy, i.e. the coupling coefficients c_i must have certain symmetries. These are called the *Manley-Rowe relations* [26] and state that the change in energy of each wave is directly proportional to its frequency. Thus, the way the waves can exchange energy is limited, with the effect being that one can consider them exchanging energy similar to quantum theory, one wave quanta at the time. This is also hinted at by Eq. (2.18).

2.5 Manley-Rowe relations for quantum hydrodynamics

If we denote the total energy density of each wave $W_{(i)}$, then the Manley-Rowe relations can be written as

$$\frac{1}{\omega_{(3)}}\frac{\mathrm{d}W_{(3)}}{\mathrm{d}t} = -\frac{1}{\omega_{(1)}}\frac{\mathrm{d}W_{(1)}}{\mathrm{d}t} = -\frac{1}{\omega_{(2)}}\frac{\mathrm{d}W_{(2)}}{\mathrm{d}t}. \tag{2.23}$$

Thus, the change in energy of each wave is proportional to its frequency. The Manley-Rowe relations are fulfilled for all the common plasma equations, e.g. the Vlasov equation and the fluid equations described previously. The fact

that an equation fulfil the Manley-Rowe relations is related to an underlying Hamiltonian mathematical structure [27, 28].

For a physical theory to be sound, one often demand it to fulfil a number of relations, such as conservation of energy, momentum and angular momentum. In Paper I [29], we consider the Manley-Rowe relations as an additional criteria in separating physical from unphysical models, in order to verify the form of the *Bohm de Broglie* term in quantum hydrodynamics. The momentum equation (here in SI units),

$$\left(\frac{\partial}{\partial t}+\mathbf{v}\cdot\nabla\right)\mathbf{v}=\frac{q}{m}\left(\mathbf{E}+\mathbf{v}\times\mathbf{B}\right)-\frac{\nabla P}{nm}+\frac{\hbar^2}{2m^2}\nabla\left(\frac{1}{\sqrt{n}}\nabla^2\sqrt{n}\right) \tag{2.24}$$

with the Bohm de Broglie term (right most term) represents the simplest quantum hydrodynamic equation [30–32]. The Bohm de Broglie term is usually small and can be neglected, but for high density, low temperature plasmas [31] it is of importance. Eq. (2.24) can be derived in several ways [32, 33], but none with total mathematical rigour.

We find the Manley-Rowe relations for quantum hydrodynamics, but starting from a more general form of the Bohm de Broglie term

$$\frac{\hbar^2}{2m^2}\nabla\left(\frac{1}{n^\xi}\nabla^2 n^\xi\right) \tag{2.25}$$

with the hope of showing that this is only valid for the case $\xi = 1/2$. From an expression for the total energy of the wave (given by electric, magnetic, kinetic, pressure and Bohm de Brogile contributions) as

$$\begin{aligned}W_{(i)}=&\frac{\epsilon_0}{2}\mathbf{E}_{(i)}\cdot\mathbf{E}^*_{(i)}+\frac{1}{2\mu_0}\mathbf{B}_{(i)}\cdot\mathbf{B}^*_{(i)}\\&+\sum_s\left[\frac{m_s n_{0s}}{2}\mathbf{v}_{(i)s}\cdot\mathbf{v}^*_{(i)s}+\left(\frac{\gamma_s P_{0s}}{2n_{0s}^2}+\frac{\xi\hbar^2k_{(i)}^2}{4m_s n_{0s}}\right)n_{(i)s}n^*_{(i)s}\right]\end{aligned} \tag{2.26}$$

we derive expressions for the change in energy of each wave. After some lengthy algebra we arrive at the main result, here expressed for wave 3,

$$\begin{aligned}\frac{\mathrm{d}W_{(3)}}{\mathrm{d}t}=\omega_{(3)}\sum_s\Bigg[&-\frac{im_s}{2}\Big(n_{(1)s}\mathbf{v}_{(2)s}\cdot\mathbf{v}^*_{(3)s}+n_{(2)s}\mathbf{v}_{(1)s}\cdot\mathbf{v}^*_{(3)s}\\&+n^*_{(3)s}\mathbf{v}_{(1)s}\cdot\mathbf{v}_{(2)s}\Big)-\frac{i\gamma_s(\gamma_s-2)P_{0s}}{n_{0s}^3}n_{(1)s}n_{(2)s}n^*_{(3)s}\\&+\frac{i\xi\hbar^2}{8m_s n_{0s}^2}\left[k_{(1)}^2+k_{(2)}^2+k_{(3)}^2-(2\xi-1)\mathbf{k}_{(1)}\cdot\mathbf{k}_{(2)}\right]n_{(1)s}n_{(2)s}n^*_{(3)s}\\&-\frac{m_s\omega_{cs}}{2\omega_{(3)}}n_{0s}\left(\frac{k_{(2)z}}{\omega_{(2)}}-\frac{k_{(1)z}}{\omega_{(1)}}\right)\mathbf{v}^*_{(3)s}\cdot\left(\mathbf{v}_{(1)s}\times\mathbf{v}_{(2)s}\right)\Bigg]+\text{c.c.}\end{aligned} \tag{2.27}$$

Even if it is not entirely trivial to see, all terms except the one proportional to $(2\xi-1)$ are symmetric with respect to the different waves, thus fulfilling

the Manley-Rowe relations, Eq. (2.23). For the Manley-Rowe relations to hold in general, that term must be 0, and thus $\xi = 1/2$ as is the case in the Bohm de Broglie term. This adds further weight to the derivation and physical soundness of the equations for quantum hydrodynamics. The fact that the Manley-Rowe relations is only fulfilled for the case of $\xi = 1/2$ also demonstrates that the Manley-Rowe relations is a useful criterion for separating physical equations from unphysical ones.

Chapter 3

Radiation and radiation reaction

In classical theory electromagnetic radiation comes in the form of waves, generated from accelerated charges. This is in contrast to quantum theory, where it is considered a particle, the photon, with the energy of each photon proportional to its frequency according to $E = \hbar\omega$ where $\hbar$ is the (reduced) Planck's constant and $\omega = 2\pi f$ the (angular) frequency. These represent different behaviour of light depending on the situation, and our attempts to connect these to macroscopic analogies. We will later see that this is resolved in *quantum electrodynamics* (QED), the most accurate description of light and matter interaction.

In this chapter we are concerned with radiation from single particles. This is in contrast to collective radiation, where particles radiate together. For particles to radiate collectively they must be close together compared to the wavelength of the emitted radiation. Considering the average particle distance as $\lambda_N = n^{-1/3}$ where n is the number density, $\lambda < \lambda_N$ represent single particle radiation and $\lambda > \lambda_N$ collective radiation. In Chapter 4, we will see that the collective radiation is what is modelled by the classical particle-in-cell scheme. The single particle radiation on the other hand is not included and where this is of importance its effects must be added.

An expression for emitted radiation from a charged particle can be derived from Maxwell's equations by considering fields which does not fall of too quickly, allowing them to propagate long distances. The result involves an integral over the full path of the particle. For relativistic particles, moving at velocities close to the speed of light, the situation is initially simplified. The radiation is predominantly due to acceleration in the *transverse* direction of motion, and the radiation is emitted in a small angle $\theta \sim 1/\gamma$ along the direction of propagation of the particle. This is visualized in Fig. 3.1.

The higher the energy of the particle and the greater the field which provide the accelerating force, the larger the power of the emitted radiation.

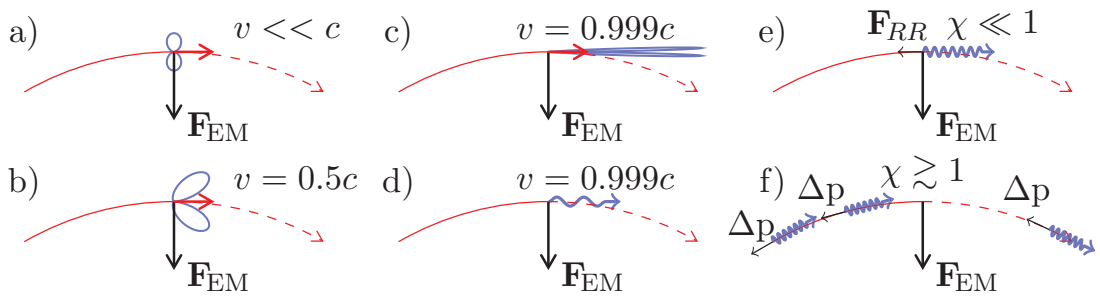

Figure 3.1: Illustration of different radiation regimes from a charged particle subject to an external perpendicular force, showing angular distribution of radiation. For low velocity (a) the radiation is emitted perpendicularly to the particle motion. As the velocity approach c (b) the distribution is tilted in the forward direction and as $v \sim c$ (c-) the radiation is emitted in the forward direction, which we visualize by a wavy arrow (d). For high γ the radiation reaction is non-negligible and can be modelled as a continuous force, but when the energy of the emitted photons approach the energy of the particle $\chi \sim 1$ the emissions must be modelled as stochastic events.

The emission results in a loss of energy for the emitting particle. This is often small compared to the kinetic energy of the particle and thus neglected, e.g. in the derivation of the very expression for how the particle emits! However, for high energy particles and large accelerating fields this energy loss, called the *radiation reaction* is not negligible and must be accounted for. This proves to be troublesome for classical theory, which breaks down; yielding unphysical solutions in which an accelerating particle can self-accelerate and which depend on the initial acceleration of the particle. There exist approximate solutions which are valid as long as the emitted radiation is small compared to the kinetic energy of the particle [34, 35]. To first order these give identical results, but they differ in higher order terms which begs the question of which are correct, in the sense of being consistent with QED [36]. Furthermore, they all have a limited range of application. For particles loosing a substantial part of their energy in radiation, the situation must be described by QED. Here emission is no longer a continuous phenomenon, but a stochastic one where there is a certain probability for photon emission.

As will be discussed, calculating these probabilities is very complicated and essentially involves summing over any possible combination in which some particles can interact. For every theory it is important with experimental validation. Recently the first experiments where conducted which showed that present laser systems can be used to measure radiation reaction, and possibly distinguish between the classical and quantum regimes [37, 38].

In the following sections we look in more detail on the theory for EM radiation and radiation reaction. This will lay the foundation from which we consider extensions to enable numerical simulations of the high intensity

laser plasma interaction regime in Chapter 4. We derive an expression for emission of *synchrotron radiation* which is applied in Paper III, V and VI in a Monte Carlo model to account for high frequency radiation. We consider a classical expression for radiation loss which is applied in Paper VI to consider the effect on radiation reaction in laser wakefield accelerations and we consider the case of radiation reaction in QED which is compared to the case of classical radiation reaction in Paper III to examine experimental signatures of radiation reaction.

3.1 Electromagnetic theory

The origin and evolution of electric and magnetic fields are described by Maxwell's equations, Eqs. (2.7-2.10). There is a solution of Maxwell's equations in vacuum where oscillating transverse electric and magnetic fields propagate as a wave with velocity $c \approx 3 \times 10^8$m/s, the speed of light. The wavelengths of this radiation can vary greatly, with e.g. radio waves in the *kilometer* (10^3 m) wavelength scale and gamma rays in the *picometer* (10^{-12} m) wavelength scale. These waves are generated by the acceleration of charged particles.

Given the path of a charged particle the radiation it emits can be calculated. The power emitted per unit solid angle and unit frequency interval is given by [39]

$$\frac{\mathrm{d}^2 I}{\mathrm{d}\omega \mathrm{d}\Omega} = \frac{e^2}{4\pi^2 c}\left| \int_{-\infty}^{\infty} \frac{\mathbf{n} \times [(\mathbf{n} - \boldsymbol{\beta}) \times \dot{\boldsymbol{\beta}}]}{(1 - \boldsymbol{\beta} \cdot \mathbf{n})^2} \exp(i\omega(t - \mathbf{n} \cdot \mathbf{r}(t)/c))\mathrm{d}t \right|^2 \tag{3.1}$$

where $\mathbf{n}$ is a unit vector in the direction toward the observer, $\boldsymbol{\beta} = \mathbf{v}/c$ is the particle velocity and $\mathbf{r}(t)$ is the position of the particle over time. This equation is in the form of an integral over all time (of nonzero acceleration $\dot{\boldsymbol{\beta}}$ where the dot denotes time differentiation) and is not suitable to use in numerics, for several reasons. First of all it is very computationally expensive to save particle positions for all time-steps, and secondly this also prevents real time calculation of the emitted radiation.

It turns out that the numerical implementation of Eq. (3.1) can be simplified for the case of *relativistic particles*, whose velocity is close to c. When the particle velocity v approach the speed of light c, Newtonian theory is no longer valid and one must take effects of special relativity into account. This states that no massive particle can surpass the speed of light, c. However, a particle with velocity very close to c can still be further accelerated to increase its kinetic energy, $E_k = mc^2(\gamma - 1)$ where the *Lorentz factor* γ is given by

$$\gamma = \frac{1}{\sqrt{1 - \frac{v^2}{c^2}}}. \tag{3.2}$$

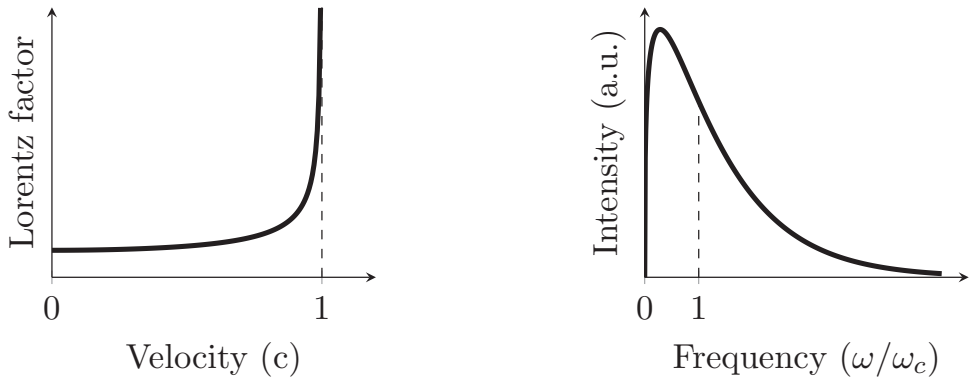

Figure 3.2: Lorentz factor (left) increasing quickly as the velocity approach the velocity of light, and the radiation spectrum of a particle emitting synchrotron radiation around the typical frequency of synchrotron radiation ω_c (right).

For non-relativistic particles this is very close to unity, but for particles approaching c it grows very quickly, as seen in Fig. 3.2. The emission from relativistic particles is concentrated within an angle $1/\gamma$ about its propagation direction. For relativistic particles with $\gamma \gg 1$ we can then to a good approximation consider all radiation as emitted along the propagation direction, removing the angular dependence from the equations. Furthermore, radiation emitted due to *transverse* acceleration ($v \perp a$) is a factor γ^2 greater than that due to *linear* acceleration ($v \parallel a$). This means that for relativistic particles the radiation due to linear acceleration can be neglected [39, 40] and one can consider all the radiation of the particle to be due to transverse acceleration. This opens up the possibility of describing the radiation from a relativistic particle by considering it to be in an instantaneous circular motion, with radius r and circular frequency ω_H.

3.1.1 Synchrotron radiation

Synchrotron radiation is the name for the typical broad frequency radiation first detected in synchrotrons, i.e. from particles accelerated in a circular motion with $v \perp a$. However, as discussed above, for a relativistic particle in an arbitrary field the contribution from longitudinal acceleration to radiation emission is a factor $1/\gamma^2$ smaller and generally negligible. Thus, it turns out synchrotron radiation is a good representation for radiation from a relativistic particle in general.

To study the phenomenon we can consider the simple example of a charged particle gyrating in an external magnetic field, a situation shown in Fig. 3.3. However, as mentioned this can be applied to a relativistic particle in general. For relativistic particles the emitted radiation is strongly peaked within an angle of $\theta = 1/\gamma$ around the propagation direction of the particle. For an outside observer, this radiation will only be visible during the short time in which the beam direction from the turning particle is within

the small angle θ towards the observer, which will register a short burst of radiation. As it is short, this must necessarily be composed of a broad range of frequencies.

We consider an electron going around in a circle of radius r with velocity v. The angular frequency is then given by $\omega_H = v/r$. For a non-relativistic electron the typical frequency of the emitted radiation is $\sim \omega_H$. However, as the particle becomes relativistic the typical frequency of the emitted radiation is instead ω_c, defined as [40]

$$\omega_c = \frac{3}{2}\omega_H \gamma^3, \tag{3.3}$$

which is greatly increased for relativistic particles with $\gamma \gg 1$. The factor $3/2$ is a matter of convention.

The rotation of the particle can be thought of as being due to a perpendicular external magnetic field H_{eff} of field strength

$$H_{\text{eff}} = \frac{\gamma m c \omega_H}{e}, \tag{3.4}$$

representing the perpendicular magnetic field which would give the same acceleration as the combined effect of the electric and magnetic fields due to the Lorentz force, with m being the mass of an electron and e the elementary charge. The frequency spectra of the emitted radiation can then be written as

$$\frac{\partial I}{\partial \omega} = \frac{\sqrt{3}}{2\pi}\frac{e^3 H_{\text{eff}}}{mc^2} F\left(\frac{\omega}{\omega_c}\right) \tag{3.5}$$

where $F(\xi)$ is the *first synchrotron function* [39, 40] given by

$$F(\xi) = \xi \int_{\xi}^{\infty} K_{5/3}(\xi')\mathrm{d}\xi' \tag{3.6}$$

with $K_{5/3}(\xi)$ being a modified Bessel function. This is such that most of the radiation is emitted around the typical frequency ω_c, as seen in Fig. 3.2. Integrating this over all frequencies we get the total radiated power as

$$I = \frac{4e^3 H_{\text{eff}} \omega_c}{9mc^2} = \frac{2e^4 H_{\text{eff}}^2}{3m^2 c^3}\gamma^2. \tag{3.7}$$

For a fixed field H_{eff} the power scales as γ^2, thus being dominated by high energy particles.

3.2 Classical radiation reaction

As a particle emits EM radiation is loses energy. As seen in Eq. (3.7), this grows as the square of both the Lorentz factor γ and the field strength H_{eff}. In the non-relativistic case this energy is extremely small compared

to the kinetic energy of the particle and can be neglected. For relativistic particles this no longer is the case, and for highly relativistic particles the emitted energy can be a substantial part of the particle kinetic energy and the energy loss must be taken into account in the motion of the particle. This is the radiation reaction and it has long been a problem how this should be accounted for. In fact, this is where classical electrodynamics fails and for a proper handling one must turn to QED. Even so, there still exist a regime where the effects of radiation reaction can be considered classically. The energy loss due to radiation reaction is then relatively small compared to the kinetic energy of the particles and the radiation reaction loss can be considered as a continuous friction term (compared to QED where there is a probability of emission, and the process is stochastic). Considering the classical case, one can add a term for the energy loss due to radiation reaction to the equation of motion of the particle

$$F = F_{\mathrm{EM}} + F_{\mathrm{RR}}. \tag{3.8}$$

We thus split the Lorentz force into an external part, F_{EM}, and a part related to the energy loss, F_{RR}. The expression for F_{RR} is then given from demanding that the work performed is the same as the energy of the emitted radiation. This gives the Abraham-Lorentz equation [39] which has the problem of containing a third order derivative. This is untypical in physics and means that is it not enough to specify the initial position and velocity of the particle for the problem to be properly defined, as is customary. Furthermore, it allows "runaway solutions", where the particle would be continuously accelerated even without an external force! This is clearly unphysical, but the problem can be removed by approximating the third order derivative using the Lorentz force, F_{EM} for the acceleration. The result is the *Landau-Lifshitz* (LL) equation, valid for $|F_{\mathrm{RR}}| \ll |F_{\mathrm{EM}}|$ in the instantaneous rest frame of the particle. In relativistic covariant form this is given by [40]

$$f^{\mu} = \frac{2}{3}\frac{er_0}{c}\partial_{\gamma}F^{\mu\nu}u_{\nu}u^{\gamma} + \frac{2}{3}r_0^2\left[F^{\mu\alpha}F_{\alpha\nu}u^{\nu} + (F_{\nu\alpha}u^{\alpha})(F^{\nu\beta}u_{\beta})u^{\mu}\right] \tag{3.9}$$

where $F^{\mu\nu}$ is the electromagnetic field tensor and $r_0 = e^2/m_e c^2$ is the so called "classical electron radius". In three vector form this becomes

$$\begin{aligned}\mathbf{F}_{\mathrm{rad}} = \frac{2}{3}\frac{r_0 e}{c}\gamma\Bigg[&\left(\frac{\partial}{\partial t} + \mathbf{v}\cdot\boldsymbol{\nabla}\right)\mathbf{E} + \frac{1}{c}\mathbf{v}\times\left(\frac{\partial}{\partial t} + \mathbf{v}\cdot\boldsymbol{\nabla}\right)\mathbf{H}\Bigg] \\ &+ \frac{2}{3}r_0^2\Bigg(\mathbf{E}\times\mathbf{H} + \frac{1}{c}\Big[\mathbf{H}\times(\mathbf{H}\times\mathbf{v}) + (\mathbf{v}\cdot\mathbf{E})\mathbf{E}\Big] \\ &- \frac{\gamma^2}{c}\left[\left(\mathbf{E} + \frac{1}{c}\mathbf{v}\times\mathbf{H}\right)^2 - \left(\frac{\mathbf{E}\cdot\mathbf{v}}{c}\right)^2\right]\mathbf{v}\Bigg).\end{aligned} \tag{3.10}$$

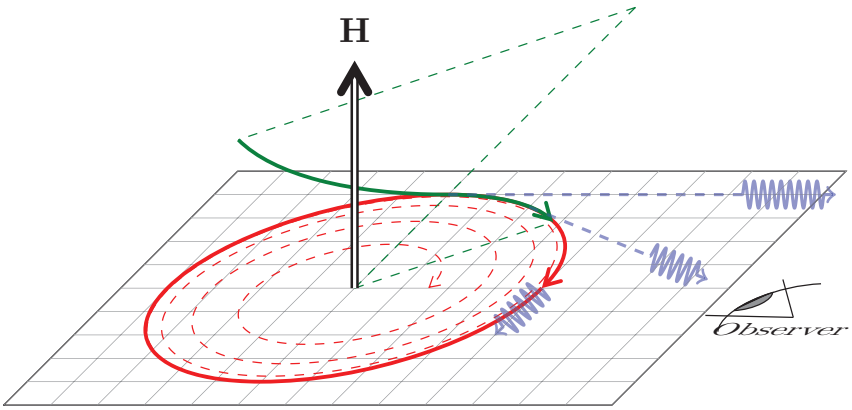

Figure 3.3: Particle gyration in an external magnetic field, without (solid red) and with (dashed red) accounting for energy loss through radiation. Green represents the path of a particle, seen as going in an instantaneous circular motion with the radii in dashed green. The radiation (blue) is emitted in a small angle along the propagation direction and an observer will register a short burst of broadband radiation.

The term on row 2 and 3 are quadratic in terms of the fields **E** and **H** and are the dominating terms for strong fields.

3.3 Quantum radiation reaction

If the energy of the gyrating particle we considered in Section 3.1.1 is further increased, then eventually the typical energy $\hbar\omega_c$ of the emitted photons will be comparable to the kinetic energy of the particle. For classical synchrotron emission this can be described by the dimensionless parameter [41]

$$\chi = \frac{2\hbar\omega_c}{3\gamma mc^2}, \tag{3.11}$$

which represent the fraction of the typical emitted photon energy over the energy of the particle.

For $\chi \ll 1$ the classical theory is valid, but for $\chi \gtrsim 1$ one must turn to QED. The problem with the classical expressions are two. Firstly, the classical equations of photon emission does not provide a proper cutoff and will eventually predict the emission of photons with greater energy than the energy of the particle itself. Secondly, the emission can no longer be considered a continuous process, but must be treated as stochastic events. This can be seen by considering the total power of emission and the typical photon energy. Radiation can only be emitted in packages, photons, and as these grow in energy the time between their emissions must grow. We can consider the time between emissions as

$$\tau = \frac{\hbar\omega_c}{I} \tag{3.12}$$

where $\hbar\omega_c$ again is the typical energy of an emitted photon and I the total power of the radiation. When considering a physical experiment, e.g. a laser pulse interacting with a plasma, how τ compares to other timescales determine if the radiation reaction can be considered a continuous friction force or a collection of stochastic events. In the QED regime, the emitted photon energy takes a substantial part of the particle energy, and the average time between emissions is larger than the typical timescale of the considered problem. In this regime the energy loss can not be considered a continuous process but must be treated as a stochastic process with a certain probability of emission. Thus, a particle, even if it is accelerated, could propagate without emitting radiation for some distance and then emit a substantial part of its energy at some instance. This is in contrast to the classical case where the radiation can be considered as emitted continuously, and results in a different dynamics for the particles (even in the classical regime the time between emissions can be larger than the timescale of the problem, but as the photon energy is so small this can not affect the particle motion substantially). According to QED one could imagine a particle moving further into a region of intense electric and magnetic fields (i.e. the focus of a laser pulse) than it would according to the classical theory, as it in each instant is not certain to lose energy due to radiation. In Paper II [42] we consider a relativistic electron colliding with an intense laser pulse and examine the difference in the radiation patterns depending on if the classical- or the QED equations for the particle motion and energy loss are used. This will be considered in more detail in the next section.

In Section 4.4, we will consider additional QED effects, not directly connected to photon emission. A high energy photon, with energy more than $2m_ec^2$ where m_e is the electron mass, can under certain conditions decay to a less energetic photon and a pair consisting of an electron and a positron. This *pair production* is a pure QED effect which does not occur in the classical description. Whereas the radiation reaction occur even for classical particles (but is negligible), pair production can not occur for low energy photons as they lack the energy to produce the pairs. Furthermore, the described process can not occur in vacuum since a single photon can not decay to an electron-positron pair due to energy and momentum conservation. However, when interacting with the low energy photons of a laser pulse this can occur. In Paper IV [43] we consider the numerical implementation of stochastic QED radiation reaction and the creation of pairs from energetic photons interacting with the laser pulse, further described in Section 4.4.

3.4 Classical v. quantum radiation emission.

In Paper II [42] we numerically consider the difference between classical and QED modelling of the radiation emission in the interaction between a single

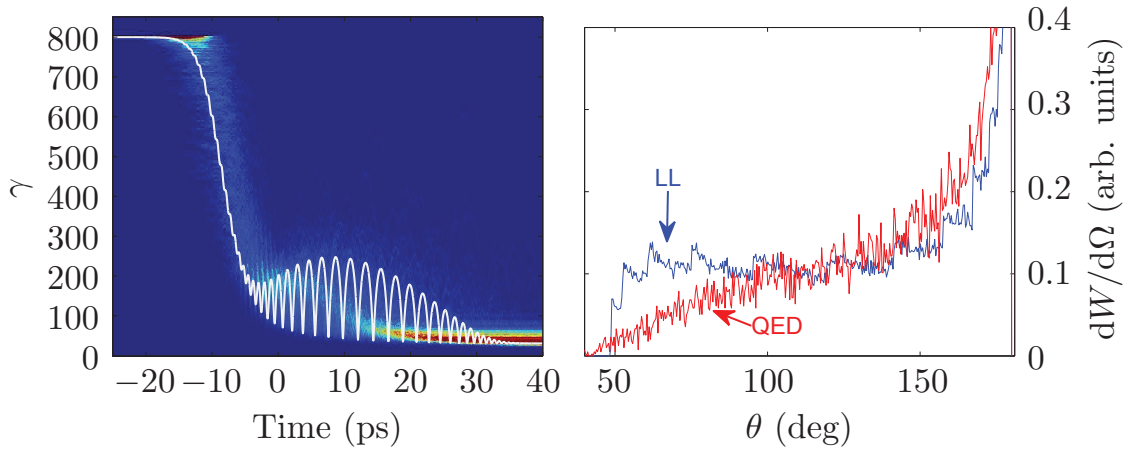

Figure 3.4: From [42]. The left panel shows the gamma value of the electron as a function of time, as it collides with the laser pulse. The white line is for a classical equation of motion and the heat map (blue to red) is from a number of QED runs. The initial electron γ value is 800 and the final value is around 50. In the QED runs the electrons penetrate further into the pulse before losing energy and their final energy is larger. The right panel shows a comparison between the angular spectra for the QED and classical (LL) case.

particle and a strong laser pulse. We make use of developed schemes for calculation of radiation, described above and which numerical implementation will be further presented in Chapter 4, with the schemes implemented in the single particle code *Simla* [44]. Here we consider only one particle interacting with an intense laser pulse. The contribution of this single particle to the fields is negligible and instead of self consistently solving Maxwell's equations (as e.g. done in the particle-in-cell scheme), here we use analytical expressions for the field of the laser pulse. This gives the possibility of modelling realistic laser pulses with variable time-steps (small when necessary in critical moments of the interaction) for the particle motion, yet keeping the required computational time modest.

Simla allows for simulation using either a classical or a QED corrected equation of motion for the particle. The quantum version uses equations for emission from QED together with (pseudo)random numbers to model emission. The effect is that the particle does not lose energy continuously as in the classical case, but rather in discrete emissions. A particle can then propagate a certain distance without radiating, and then emit a large part of its energy as radiation during one time-step. This process is not deterministic, and we run a large number of QED runs to get a representative picture of the process.

We consider the head-on collision between a laser pulse and an electron. As a first step the laser pulse is given by an ideal Gaussian shape with relativistic amplitude $a_0 = 200$, with the electron having $\gamma = 800$. As the electron meets the pulse its energy is decreased, as can be seen in Fig. 3.4.

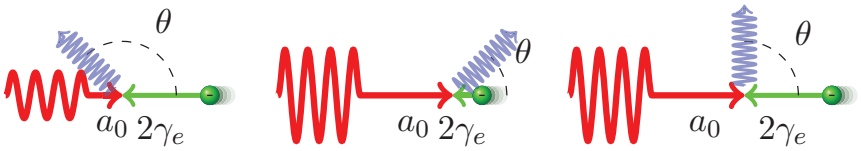

Figure 3.5: Illustration of the direction of predominant radiation emission, θ, for different laser field strength a_0 and electron energy γ_e.

Here one can also see that the electron Lorentz factor γ is generally underestimated in the classical case compared to the QED case: the electrons penetrate further into the laser pulse before loosing energy and the energy of the electrons after the collision is greater. The resulting angular spectrum of the radiation can be seen in Fig. 3.4, where one can see that the energy for smaller θ is overestimated by the classical case (here θ represent the angle compared to the propagation direction of the laser pulse).

To understand this effect one must consider the typical direction of radiation emission. It is such that for $a_0 \ll \gamma$ the radiation will be emitted in the forward direction of the electron propagation, for $a_0 \gg \gamma$ it will be emitted in the opposite direction (of the initial electron propagation direction) and for $a_0 = 2\gamma$ the predominant direction of emission is perpendicular to the (initial) electron propagation direction [45], see illustrations in Fig. 3.5. Thus, for a given pulse amplitude a_0, the smaller γ is, the more the radiation will be concentrated to smaller angles θ (towards the propagation direction of the laser pulse). Because the electron energy is underestimated in the classical case, as seen in Fig. 3.4, more energy will be emitted for small θ than in the corresponding QED case. The described effect was for the idealised case of a Gaussian shaped pulse together with a single electron. To see that the observed effect is robust enough to be observed in an experiment we also consider the case of a realistically shaped pulse with a beam of electrons with a spread in energy and position. The result is that indeed, the effect is present also here and thus could work as a signature for an experiment probing radiation reaction.

Chapter 4

Particle-in-cell method

4.1 Classical particle-in-cell scheme

The particle-in-cell (PIC) scheme is a method of plasma simulations [19, 20] which has become a standard tool for large scale plasma simulations. Here the plasma consists of an ensemble of particles moving within a grid representing the simulated space. To advance the system in time, Maxwell's equations (Eqs. (2.7) - (2.10)) for the electric- and magnetic field in each grid point and the equation of motion for the particles are solved self consistently.

There are different numerical methods for the field solver (e.g. FDTD [20, 46] or spectral [47] methods) and the position of each component of the field can vary within the grid cell, but for all cases the fields are considered to be placed discretely on the grid, with particles moving continuously (up to computer number precision) there in.

The steps in the method can be seen in Fig. 4.1. For each particle and iteration the position and velocity of the particles are weighted to the grid to get the charge- and current densities $\rho(\mathbf{r})$ and $\mathbf{J}(\mathbf{r})$. These are then used in Maxwell's equations in order to update the values of the E- and B-fields. Finally, the field values are weighted to the positions of each particle and the equation of motion is solved in order to update the position and momentum of the particles, after which the process restarts for another iteration. In a typical simulation the number of particles under consideration is much too great to include all in the simulation, due to the computational workload as well as memory limitations (e.g. the 10^{15} particles in 1 mm^3 of a typical gas would require $\sim 5 \times 10^4$ TB of memory to store the position and momentum of each particle). In PIC one instead consider *super-particles*, each representing a larger number of real particles. These super-particles are considered to have a finite size and will partially overlap when calculating the charge- and current densities. Given a certain field the super-particles follow the same path as real particles would do, as the charge to mass ratio is the same. The equation of motion for the particles is given by the Lorentz

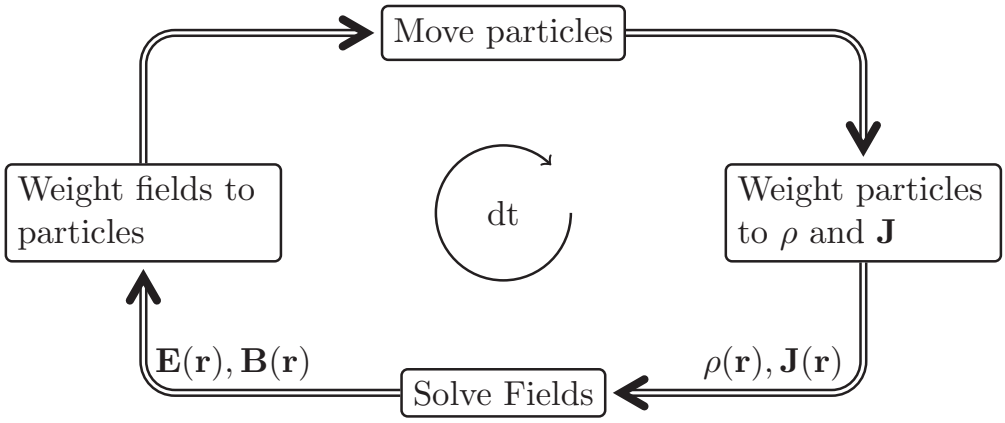

Figure 4.1: The classical particle-in-cell scheme. Particles are weighted to the grid to create charge- and current densities ρ and $\mathbf{J}$. These are used to update the fields $\mathbf{E}$ and $\mathbf{B}$ which are weighted back to the particle positions. The particles finally move and the next iteration starts.

force, $F = q(\mathbf{E} + \mathbf{v}/c \times \mathbf{B})$, where the *Boris scheme* [48] is the most common *particle pusher*. This is an efficient leap-frog method where first half the acceleration due to the electric field is applied, then a rotation due to the magnetic field and finally the other half of the contribution due to the electric field.

The PIC method has turned out to be applicable for plasma simulations in a large number of regimes, with the original method extended to include e.g. collisions [49] and ionization [50]. However, present and coming [51–53] high intensity laser facilities present regimes where the PIC method fails to take into account the emission of high frequency radiation, prompting extensions for this and the corresponding radiation reaction [54, 55]. For even further increase in intensity other problems will arise, related to the fundamental change of physics as *quantum electrodynamics* (QED) have to be considered.

4.2 Particle-in-cell extensions

Planned high power laser facilities[51–53] will see the peak laser intensity move towards $10^{23}\mathrm{W/cm}^2$. These pulses are capable of accelerating electrons to relativistic velocities within a single wavelength. As seen in Eq. (3.3), $\omega_c = \frac{3}{2}\omega_H\gamma^3$, the frequency of the emitted radiation is greatly increased for relativistic particles with $\gamma \gg 1$, and correspondingly the wavelength is decreased.

This poses a problem to the PIC scheme. Not only is there an issue that the spatial and temporal resolutions $\mathrm{d}x$ and $\mathrm{d}t$ provide a cutoff for the radiation that can be resolved by the grid, such that radiation with wavelength $\lambda \leq \mathrm{d}x$ (or frequency $f \geq 1/\mathrm{d}t$) can not be resolved. There is also the fundamental problem that the PIC scheme would not reproduce the

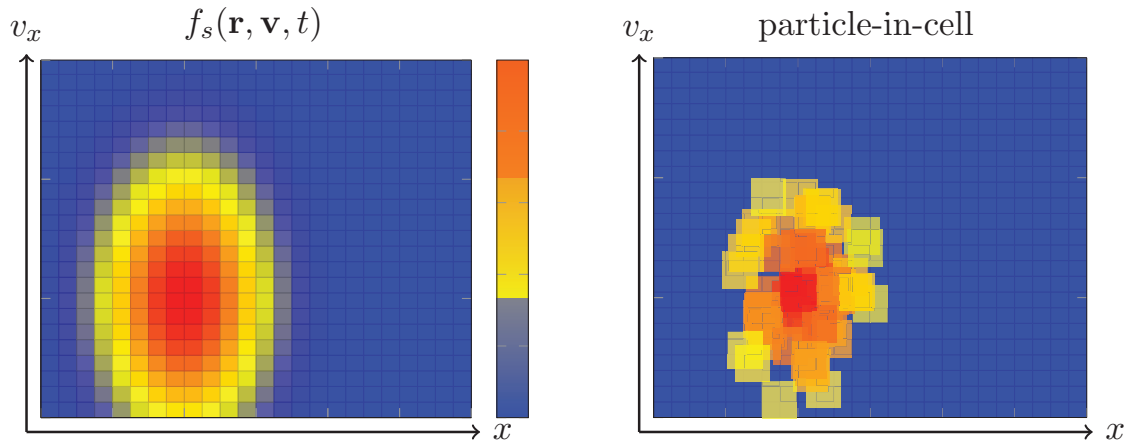

Figure 4.2: Illustration of the particle-in-cell method compared to the distribution function $f_s(\mathbf{r}, \mathbf{v}, t)$ from kinetic theory in Section (2.2.1). The distribution function can be considered as sampled on the PIC grid, with little computational effort spend on empty regions.

correct radiation, even if the grid resolution was greatly improved. This is related to the fact that the PIC idea is to use super-particles, representing a large number of real particles. As they have the same charge-to-mass ratio as real particles they follow the same path as the effect of the Lorentz force is the same. However, not all equations have this simple dependence on charge over mass, with e.g. the intensity of the high frequency radiation in Eq. (3.7) scaling as e^4/m^2. The emission of high frequency radiation can be seen as a single particle, microscopic effect that is not taken into account by the PIC scheme, which instead focus on the collective, macroscopic behaviour of the plasma. In order to include this physics the PIC scheme must be extended.

In Section 4.3, we consider a method of accounting high frequency EM radiation, not resolved by the grid, in the form of particles. This is a classical expression, and we use a statistical routine to sample from the spectrum, determining the emission using pseudo-random numbers (a Monte Carlo method). Counted over a large amount of particles, this gives a good description of the emitted radiation.

In Section 4.4, we consider extensions to the PIC methods to enable simulations of regimes where QED effects starts to be of importance. This includes the emission of high frequency radiation, but also pure QED effects which have no classical equivalent, such as pair production. The methods for accounting for radiation emission and pair production are Monte Carlo methods as well, but based on QED cross sections. And more importantly, here also the underlying physics is stochastic with the QED cross sections providing probabilities of photon emission and pair production.

In the following sub-section we consider the classical and QED descriptions of EM radiation and how this relate to the description of radiation in PIC as a field on the grid or as particles in the form of classical or QED

"photons".

4.2.1 Different descriptions of EM radiation

Classically EM radiation was considered to be a wave, exhibiting wave like properties such as interference in two-slit experiments. Here light going through two nearby slits not only add up, but interfere such that there are spots on the screen behind where the intensity of light is smaller when both slits are open than when one of them is closed. Electrons and protons on the other hand has been considered particles, exhibiting particle like properties such that they come in discrete packages. However, it turned out that there were situations in which the wave description for EM radiation was insufficient and light instead had to be considered as particles, e.g. to explain the cut-off frequency in the *photoelectric effect*. Here light is shone at a metal which then emits electrons as it absorbs the energy of the light. However, below the cut-off frequency no electrons are emitted, independent of the intensity of the light, indicating that the energy is passed in discrete packages, with energy proportional to their frequency. Likewise, classical particles such as electrons and protons turned out to have wave like properties in certain situations, such as interference in two slit-experiments as mentioned above (though with very small slits [56]). This insufficiency of being able to describe these phenomena as either of these two, to us well-defined and separate, cases is resolved by QED. Here everything is considered as particles, but whose motion is governed by probabilities given by the square of a corresponding complex amplitude. This regains the discrete nature of particles at the same time as it enable the wave like properties through interference between amplitudes of different outcomes.

Thus, the notion of EM radiation as photons is a quantum description. Here, e.g. in the extensions of the PIC scheme, we will consider the high frequency radiation to be particles, and we call them "photons" in a more semi-classical fashion, using the simple relation between the frequency f of the light and the energy of the "photon" $E = hf$. It turns out that the low frequency radiation which we can resolve on the grid and the high frequency radiation which we include as particles in the PIC simulations occupy two distinct energy regions in frequency space. In the low frequency part we have the collective radiation from a large amount of particles, described by the grid. As e.g. when a laser interact with a plasma, the particles move collectively and emit radiation, e.g. with the effect of reflecting the laser pulse if the plasma is over critical. The particles must be close together compared to the wavelength of the radiation, thus on micrometer scale for optical radiation. The energy of the emission from each particle is low but this is compensated by the great amount of particles radiating collectively within this region. In the high frequency part we have the single particle emission of high frequency photons. Here the wavelength of the radiation

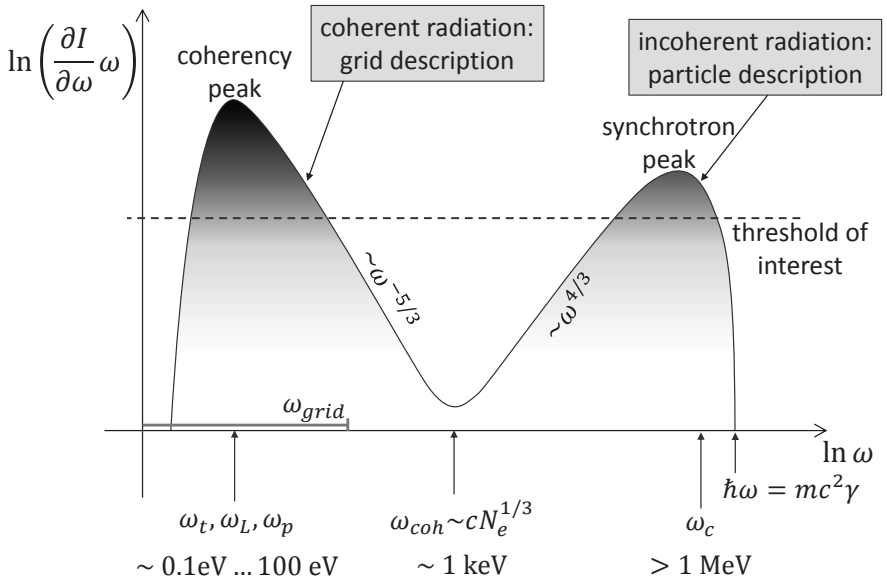

Figure 4.3: From [43]. Illustration of how the energy in typical high intensity laser matter interaction can be considered as in two regimes. The laser pulse and plasma fields constitute the coherent regime, where many particles radiate together within one wavelength. One the other side of the scale is the incoherent regime, where high energy particles emit high frequency radiation.

is very small and the radiation is emitted in small angles, and there are no collective effects. In order to radiate collectively the particles would have to be very close together both in ordinary space and velocity space, which they are typically not for our considered regimes (there is however possible to design such regimes, e.g. in the case of an *undulator*). All in all, these distinct regions of radiation, which are illustrated in Fig. 4.3, allows us to include the high frequency radiation without the double counting of the radiation being a substantial part of the total energy.

4.3 Monte Carlo method for synchrotron radiation

In order to calculate the emitted radiation from high energy particles we use a *Monte Carlo* model: We calculate the spectra according to the frequency spectra for synchrotron radiation, Eq. (3.5), and then we *sample* from this through a method involving (pseudo) random numbers. Each emission then involves picking a frequency from the spectra, and emission is determined according to how probable emission of that frequency is. This is a computationally efficient and easy to use method where we in average get the correct number of emissions for each frequency interval and can build statistics from this (e.g. frequency and angular spectra).

From values of particle position and momentum before and after the

equation of motion is applied, we can calculate what *efficient magnetic field* H_{eff} this represent. This is the magnetic field, perpendicular to the particle motion, that would cause the same transverse change in the particle momentum, and for a relativistic particle this is given by

$$H_{\text{eff}} = \frac{mc\gamma}{e}\frac{1}{\Delta t}\frac{\sqrt{\mathbf{p}^2\mathrm{d}\mathbf{p}^2 - (\mathbf{p}\cdot\mathrm{d}\mathbf{p})^2}}{\mathbf{p}^2} \tag{4.1}$$

where $\mathbf{p}$ is the momentum and $\mathrm{d}\mathbf{p}$ the change in momentum of the particle, valid when the change in momentum is much smaller than the momentum, $\Delta p_\perp/p \ll 1$. H_{eff} determines the typical frequency ω_c of the emitted radiation given by

$$\omega_c = \frac{3eH_{\text{eff}}}{2mc}\gamma^2 \tag{4.2}$$

and thus the spectra of the emitted radiation. We wish to pick a frequency ω and use the spectrum $\partial I(\omega)/\partial\omega$ to determine if a photon with such a frequency is to be emitted. We want to do this in a clever way in order to reduce noise and speed up computations. On the one hand we wish to allow for picking a wide range of frequencies, but on the other hand we do not want to pick frequencies with extremely small probability of emission too often, as this would be a waste of computational resources.

To solve this we generate ω according to a distribution function $S(\omega)$, so that frequencies for which the probability of emission are large are more often selected. This is then compensated for by decreasing the probability of emission by the corresponding values. In order to do this numerically, without resorting to tabulated values, one need a function which is easily integrable, which is not the case for the synchrotron function. However, we can construct a simplified function $S(x)$ using the asymptotic values of the synchrotron function. Thus, our simplified function approaches the values of the synchrotron function for the extreme cases of $\omega \to 0$ and $\omega \to \infty$. This function is chosen as

$$S(x) = \begin{cases} 4/3x^{1/3} & \text{if } x < a, \\ 7/9e^{-x} & \text{if } x > a, \end{cases} \tag{4.3}$$

where the constant $a \approx 0.69021$ is determined such that $\int_0^\infty S(x) = 1$. We can then calculate

$$P(\omega) = \int_0^\infty S(x)\mathrm{d}x \tag{4.4}$$

and find its inverse $\omega(P)$ such that we can pick the frequency as $\omega = \omega(R)$ where R is a (pseudo) random number $R \in [0, 1]$. The number of photons of frequency ω is then given by

$$\mathrm{d}N = \frac{\frac{\mathrm{d}I}{\mathrm{d}\omega}(\omega)}{\hbar\omega S(\omega/\omega_c)}\Delta t \tag{4.5}$$

where Δt is the time-step. If a photon should be emitted is then determined by comparing $\mathrm{d}N$ to another (pseudo) random number $R' \in [0, 1]$, where a photon is emitted if $\mathrm{d}N \geq R'$.

The scheme is limited in that it does not take interference between emission at different time-steps into account. However, the separation into coherent and incoherent emission for a many-particle system, as illustrated in Fig. 4.3, is built on the assumption that high-frequency single particle emissions are indeed incoherent, i.e. free from interference phenomena to a good approximation. For applications in high-intensity laser-matter interaction this is a reasonable assumption [57].

Also, even if the approximation used in Eq. (4.1) is generally very good for relativistic particles, situations can occur in PIC simulations where it is violated, due to the Boris scheme particle pusher. One can imagine rare events where a particle is decelerated to a low energy by the first half of the electric field, and because of this it is then greatly rotated by the magnetic field. When the final half of the electric field then is applied, the particle momentum will have turned completely. This gives a large change in momentum $\Delta p_\perp$ and a small average momentum p, greatly overestimating H_{eff} with the effect of rare, much too energetic emissions. We solve this issue by imposing the limit $\Delta p_\perp / p \leq 1$ in the calculation of H_{eff}.

We use the method of radiation emission in several papers. In Paper III [57] the method is developed and implemented into the PIC-code *ELMIS3D* [58] and we perform benchmarking against the radiation loss calculated by the Landau-Lifshitz equation, Eq. (3.10), for the case of the bubble regime [59] of laser wakefield acceleration [60, 61], described further in Chapter 5. A short, intense laser pulse is shot at an underdense plasma, with electrons accelerated in the strong plasma wake field following the pulse. The electrons are accelerated to relativistic energies [62, 63] and radiate high frequency radiation [64, 65]. In Fig. 4.4 the comparison between the energy loss of the particles as given by the radiation reaction force and the emitted energy as calculated by Eq. (4.5) can be seen, with excellent agreement between them.

4.4 QEDPIC

In Paper IV [43], we present and review particle-in-cell extensions to include important QED processes [66–69] in order to allow for PIC simulations including ultra-strong laser pulses. Under these conditions, not only can particles emit high energy radiation; but this radiation is of sufficient energy to produce electron-positron pairs when interacting with the laser, as mentioned in Section 3.3.

The QED results which are implemented into the PIC model are *scattering probabilities* [70, 71]. These represent the probability of some state of

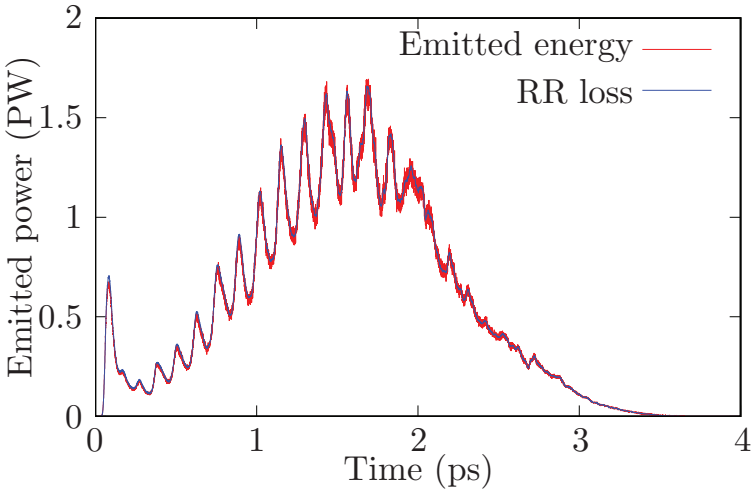

Figure 4.4: From [57]. Comparison between the energy loss due to radiation reaction (blue) and the energy of the radiation emitted by the Monte Carlo synchrotron radiation scheme (red).

particles in an (infinite) past evolving to another state of particles in some (infinite) future. Even so, the typical time scale of these QED processes (of the order 1 over the Compton frequency) are much smaller than the particle-in-cell time-step. Dividing by the (infinite) interaction time results in finite conversion rates for these processes, which can be used to determine if the process takes place for a given particle and time-step, or not. The exact solution of these probabilities are very hard to calculate, so the results are approximated by perturbation theory in QED. In principle the particles could have an arbitrary number of interactions, represented by an infinite series of interactions with ever-increasing complexity. However, to first order in perturbation theory we only consider one interaction. These interactions are suitably represented by a corresponding *Feynman diagram*, as seen in Fig. 4.5.

In *absence* of an external field, the most simple interactions in QED involves two incoming and two outgoing particles as with fewer particles one can not obtain momentum conservation. This means that e.g. an energetic electron in vacuum could not spontaneously break down to a photon and a (less energetic) electron, i.e. an electron in vacuum subject to no force will not radiate. However, this changes in the presence of an external field, e.g. an intense laser pulse. As is known, an energetic electron accelerated in such a field can radiate to form a photon, with the exchange of momentum with the external field guaranteeing momentum conservation.

In QED such situations can be described by dressed particles states, representing particles in the presence of an external field, with the most simple interactions now involving one incoming and two outgoing particles

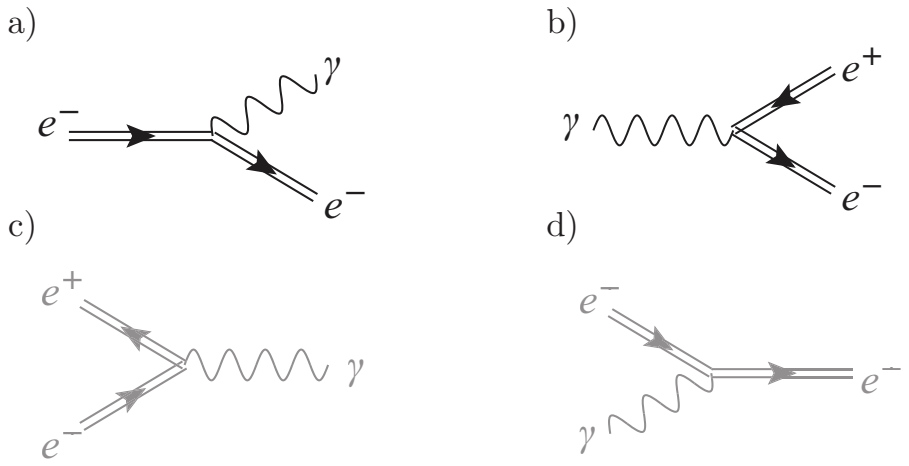

Figure 4.5: From [43]. Feynman diagrams for the included (above) and omitted (below) processes. Photon emission (a) and pair production (b) are included processes. In photon emission a single electron radiate to become a photon and a less energetic electron and in pair production a single energetic photon produce an electron-positron pair. Pair annihilation (c) and photon absorption (d) required a close collision of two particles at a small angle and can be neglected for the considered regime.

or two incoming and one outgoing particles, which can be seen in Fig. 4.5 (with the dressed states represented by double lines). There are four distinct such processes.

Two of these are essential to include for the purpose of simulating high intensity laser plasma interactions, whereas the other two turn out to be negligible for our needs.

4.4.1 Included processes

The two included processes can be seen in the top row of Fig. 4.5. The first diagram represent the emission of a high energy photon from an electron (or positron) interacting with an external field, thus subject to a force from e.g. a laser. This is similar to the classical synchrotron emission considered in the previous section, however with some important differences. Here the photon energy is limited to not exceed the energy of the particle, which would be unphysical. The corresponding spectra is given by [43, 72, 73]

$$\frac{\partial I}{\partial \omega} = \frac{\sqrt{3}}{2\pi}\frac{e^3 H_{\text{eff}}}{mc^2}(1-\delta)\left(F_1(z_q) + \frac{3}{2}\delta\chi z_q F_2(z_q)\right) \tag{4.6}$$

where $F_1(x) = x\int_x^\infty K_{5/3}(x')\mathrm{d}x'$ and $F_2(x) = xK_{2/3}(x)$ are the first and second synchrotron functions respectively and $z_q = 2/3\chi^{-1}\frac{\delta}{1-\delta}$ where $\delta = \hbar\omega/(\gamma mc^2)$ and $\chi = \frac{2}{3}\hbar\omega_c/(\gamma mc^2)$ as in Eq. (3.11). $K_{5/3}(x)$ and $K_{2/3}(x)$ are modified Bessel functions. For $\delta \ll 1$ this goes over to the classical expression in Eq. (3.5) and as $\delta \to 1$ the emitted intensity approaches 0, thus the

spectra is limited such that no photon with more energy than the radiating particle can be emitted. The classical expression is not limited in energy, and as concluded in Eq. (3.11) this expression is only valid in lower energy regimes where this is not a problem. Furthermore, the interaction between the electron and the field can be considered as the electron absorbing an arbitrary number of laser photons and then emitting a high energy photon, referred to as nonlinear Compton scattering [72, 74]. The corresponding recoil on the electron is the radiation reaction[75–78], with classical radiation reaction retrieved in the classical limit [36, 75, 79]. The second important difference is that the QED process is an intrinsically stochastic process, as discussed in Section 3.4. Thus, there is no continuous emission, but instead a probability of emission in every instance. The numerical method used is similar to the synchrotron case described in Section 4.3. We use a Monte-Carlo method to determine emission through comparison of emission probability with a pseudo-random number. However, where that process then was a method to collect statistics of the emission from a large number of particles, here this is a good representation of the physical process itself. And the radiation reaction, which for the synchrotron case still was calculated as a continuous force, is now a discrete, stochastic event.

The second diagram, (b) in Fig. 4.5, represents the emission of an electron-positron pair as a high energy ($\geq 2m_e c^2 \approx$1MeV) photon interacts with the laser field. Unlike the first diagram, this has no classical equivalent. In order to create pairs the energy of the photons must be larger than twice the rest mass of the electron, or there will be insufficient energy to create a pair. The numerical method is similar, with the cross section for the process used in a Monte-Carlo process to determine if the event takes place.

4.4.2 Omitted processes

The omitted processes can be seen in the bottom row in Fig. 4.5. Here two particles interact, resulting in a single particle. In the left diagram an electron and a positron collide to produce radiation in a process called "pair annihilation". In the right diagram an electron (or positron) absorbs a high energy photon to gain energy in "photon absorption". This can be seen as a collision between an electron and a photon and the cross sections for the two processes are similar. The reason that these processes can be omitted is that they require a collision with a close to opposite propagation direction [80]. In order for the annihilation and absorption processes to be of importance the positron/high energy photon densities must be very high, i.e. having approached some equilibrium state where the absorption and creation rates are of similar magnitude. Given typical high intensity laser-matter interactions these are highly unlikely events and can thus be neglected.

4.4.3 Higher order terms in QED

The terms in Fig. 4.5 are only the first of an infinite series of ever more complicated interactions between particles in the laser pulse. One can imagine an arbitrary number of particles in an infinite past, which through interactions can evolve into different states in an infinite future. This would of course be very hard to numerically implement. However, we argue that an important set of these processes, to a good approximation, can be seen as included by the above described first order processes. These are those that can be built from the included creation processes, however not those involving photon absorption or pair annihilation.

As an example we consider a process in which a single electron result in two electrons and a positron, a process generally referred to as the "trident". In the PIC implementation, this process can occur through the single electron first emitting an intermediate photon, with this photon then producing a pair.

Furthermore, according to QED, this can also occur without the intermediate photon ever being created. Feynman diagrams are merely a convenient method of accounting which terms to evaluate, and not a direct picture of reality. The intermediate photon is then only an internal line in a Feynman diagram which does not fulfil energy and momentum conservation, and we call it a "virtual" particle.

It turns out that both these situations (with the intermediate particle being either real or virtual) are described by the same Feynman diagram, which can be split into a real intermediate particle part and a virtual intermediate particle part [81]. For the real particle part the intermediate particle fulfils energy-momentum conservation and for the virtual particle part it does not. Note that dressed particles are required as otherwise "splitting" the Feynman diagram would produce sub-processes which give zero contribution due to lack of energy-momentum conservation.

Comparing the real and virtual part it turns out the probability of the latter is generally smaller [82]. Thus, to a good approximation we can consider higher order Feynman diagrams involving photon emission and pair creation to be included as the diagrams can be split into cases with real or virtual intermediate particles, with the real cases being included by combinations of the first order diagrams and the virtual cases being smaller than the corresponding real case.

In other words, higher order terms can be seen as approximated by the combination of lower order terms, and e.g. a cascade of particles can be formed from a single electron in a strong laser pulse, with the intermediate particles all being real.

Chapter 5

Laser wakefield acceleration

In laser wakefield acceleration (LWFA) a high intensity laser pulse is sent into an underdense plasma [60, 61]. The laser pulse perturbs the electrons in the plasma, creating a plasma wave with a phase velocity close to the speed of light following the laser pulse. In this wakefield the charge separation gives huge electric fields of the order $\sim$ 100GV/m [10, 11] (theoretically limited by the critical density for laser propagation, thus at $\sim$ 1TV/m for optical lasers), in which electrons can be trapped and accelerated to relativistic velocities. The laser, the plasma wakefield and the trapped particles all move with velocities close to c, and the electrons can gain energy for as long as the structure remains.

5.1 Conventional accelerators

The experimental problem of accelerating particles to relativistic energies was touched upon in the introduction, Chapter 1. Here we again consider this, in preparation for considering laser-plasma accelerators in the next section.

To achieve high energy particles, the accelerating fields must be large, and they must act on the particle for a long time. With particles moving at close to the speed of light c, this usually also implies that they must act for a long distance. Long distances in turn will imply large and expensive facilities. To counteract this one could of course increase the field strength, but there is a limitation for conventional accelerators in that eventually the fields will ionize the accelerator walls. Later we will see that this limitation does not exist for *plasma accelerators*, allowing for a shorter acceleration distance and thus smaller and less expensive facilities.

Another effort of efficient acceleration could be circular facilities where the particles make several passes. However, for a charged particle moving in a circle the smaller the circle and the lighter the particle, the greater fraction of its energy it will lose through radiation. This effectively limits the energy

gain and again emphasis the requirement for large facilities. Furthermore, for heavy ions the required magnetic fields needed to keep the particle in circular motion can provide a limitation.

There are three common types of accelerators. In a *linear accelerator* the particles are accelerated in a straight line. The advantage is that the energy loss through radiation is very small and will not be of importance unless the energy gain is of the order of 10^{14} MeV/m [39]. The disadvantage is the particles only make a single pass and the facility needs to be very long, as e.g. the 3.2 km long *SLAC* facility [6].

In a *cyclotron* particles are accelerated in a spiral path. A static magnetic field, perpendicular to the disk in which the particles move, keeps the particles in circular motion and the radius of their path is increased as their energy is increased. The particles gain energy through an applied alternating potential, matched with the frequency of rotation. As the particle energy increase so does the radius of rotation, and as the particles reach the outer boundary of the device they are ejected. The makes it possible for the cyclotron to provide a continuous flow of ejected particles.

In a *synchrotron* the particles are accelerated in a circular path. This is similar to the cyclotron, with the difference that the strength of the magnetic field is adjusted ("synchronized", hence the name) to the energy gain of the particles to keep the radius constant. The particles can then circulate many laps to reach very high energies, or even be "stored" at a constant energy in what is called a *storage ring*. However, unlike the cyclotron, there can be no continuous injection of particles. Instead, the particles are accelerated and then ejected in a burst. The synchrotron can also need some other device to accelerate the particles to a sufficient energy to go in the desired circular path.

5.2 Laser-plasma interaction

In a plasma the behaviour of the particles are intrinsically connected to the behaviour of the EM fields. The movement of the particles create fields and these in turn affect the motion of the particles. For a proper description these must thus be handled self-consistently. However, one can still get much insight into plasma behaviour by considering *single particle effects*, where we consider a single particle and how it behaves in certain field configurations. And since it is a single particle, its effect on the fields is negligible; considerably simplifying the situation as we can consider the fields as given and simply calculate the behaviour of the particle.

5.2.1 Single particle oscillations

A single charged particle with mass m and charge q in a given field configuration with an electric field $\mathbf{E}$ and a magnetic field $\mathbf{B}$ is affected by the

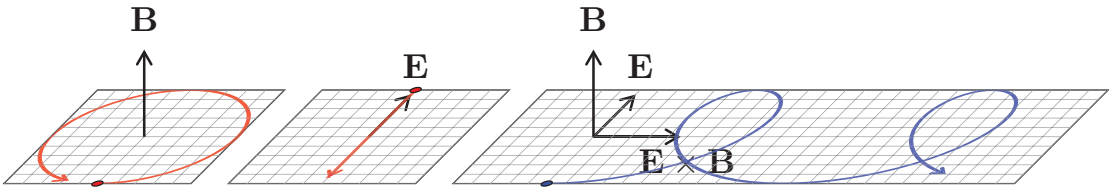

Figure 5.1: Motion of a negative charge subject to 1) a transverse magnetic field, 2) an electric field and 3) both the mentioned fields. With the combined fields the $\mathbf{E} \times \mathbf{B}$ drift results in an average motion in the $\mathbf{E} \times \mathbf{B}$ direction, independent on the sign of the charge.

Lorentz force $\mathbf{F} = q(\mathbf{E} + \frac{\mathbf{v}}{c} \times \mathbf{B})$. The magnetic field can do no work on the particle, only change its direction. Given a constant magnetic field $\mathbf{B}$ a charged particle can gyrate in the transverse plane, as seen in Fig. 5.1. An electric field $\mathbf{E}$ can accelerate a particle in the direction of the field and thereby pass energy to the particle. Given a constant electric field a charged particle would accelerate, indefinitely, in the direction of the field. However, applying both of these fields the situation is more complicated, as seen in the right panel of Fig. 5.1.

The magnetic field will try to turn the particle in circular motion. The electric field will provide positive acceleration until the particle has turned perpendicular to the E-field. Here the particle reach its highest energy with the E-field then providing deceleration until the particle energy reach its minimum after a further half lap. As the particle is turned, there is no general motion in the direction of the E-field, however the radius of the gyration depends on the particle energy and will be larger on one side than on the other. The result is that the particle path does not close to a circle, and there is a general drift, perpendicular to both the E and B-field (here it is assumed $E/B < 1$ as otherwise the drift velocity would exceed c). This is called the $\mathbf{E} \times \mathbf{B}$ drift, and is an example of a single particle drift. Similarly, in a non-uniform magnetic field the radius of a gyrating particle will depend on the strength of the magnetic field, with a stronger field able to bend the particle motion into a smaller radius. This also result in a path being non-closing circles and a general drift, here called the grad-B drift.

5.2.2 Ponderomotive force

A very important effect in laser-plasma interaction is the *ponderomotive force*. This is an effect involving a high frequency, spatially dependent electric field. In a simple model of a laser pulse, we have transverse E- and B-fields (to each other and the direction of motion) with a frequency ω and a Gaussian shape diameter and duration (pulse length). We thus have a spatial dependence where the field is strongest in the center of the pulse and then fall of in all directions.

If we consider a particle somewhere in the laser pulse, the ponderomotive

force can be visualized as follows. The particle will oscillate in the electric field. As it does, the field will be stronger to one side and weaker on the other. As the particle oscillates, it will only be able to move a small distance towards the strong field, but the kick-back will take it deep into the weak field, moving the center of oscillation with the result being a force towards the weaker part of the pulse.

In more detail, if we consider a charged particle with mass m and charge q in the field given by

$$\mathbf{E} = \mathbf{E}_0(\mathbf{r})\cos(\omega t) \tag{5.1}$$

where $\mathbf{E}_0(x)$ is the spatially dependent amplitude. The ponderomotive force is then given by

$$\mathbf{F}_p = -\frac{q^2}{4m\omega^2}\nabla(\mathbf{E}_0^2). \tag{5.2}$$

This is independent of the sign of the charge and will thus accelerate ions and electrons in the same direction. However, due to the mass dependence, the effect on the electrons will be much greater. We will soon see how this can create a cavity, void of electrons, in laser wakefield acceleration.

5.2.3 Normalized laser amplitude

A charged particle interacting with a laser pulse will be affected by the Lorentz force, depending on the E- and B-fields and the particle velocity. If the velocity is $v \ll c$ the effect of the magnetic field will be negligible and the motion will be governed by the electric field. Given the field $\mathbf{E} = \mathbf{E}_0 \exp(i\mathbf{k}\cdot\mathbf{x} - i\omega t)$ we can solve the equation for the motion of the particle as

$$\mathbf{v} = \frac{iq\mathbf{E}_0}{m\omega}. \tag{5.3}$$

Comparing this velocity to c we can get an estimation of the validity of the non-relativistic assumption $v = qE_0/m\omega \ll c$. Dividing by c, we can introduce the convenient dimensionless parameter

$$a_0 = \frac{qE_0}{mc\omega} \tag{5.4}$$

for which $a_0 \ll 1$ represent the classical, non-relativistic regime and $a_0 \gtrsim 1$ the relativistic regime. In the relativistic regime the effect of the magnetic field is not negligible and for $a_0 > 1$ we can have strongly nonlinear effects.

5.3 LWFA scheme

A focused laser pulse propagating through vacuum will not stay focused, but will spread with the distance travelled, i.e. the pulse will undergo diffraction. A measure of this is given by the *Rayleigh length*, $Z_R = \pi w_0^2/\lambda_0$, the

distance at which the laser spot size has increased a factor $\sqrt{2}$ from its minimum, where w_0 is the laser spot size (given by the radius at which the laser intensity falls of by a factor $1/e^2$) and λ_0 is the laser wavelength. Thus, the tighter the focus (smaller laser spot size) the shorter the length at which it will stay focused.

The situation is different when the pulse propagates through a plasma. The velocity of the EM wave is then dependent on the plasma frequency ω_p, and hence the plasma density and effective electron mass. When the laser pulse propagates through the plasma it perturbs the electron density with electrons expelled from the laser pulse region through the ponderomotive force, lowering the density in the laser pulse region. The resultant change in refractive index, together with the relativistic mass increase of the energetic electrons in the pulse region, can keep the laser pulse from diffracting provided the density is not too small. This *self-focusing* [83] allows for the laser pulse to propagate a long distance through the plasma, accelerating electrons trapped behind the laser pulse to high energies, up to the order of GeV [12, 63]. The critical power for self-focusing, $P_c \approx 17\omega_0^2/\omega_p^2$ [GW][83], gives an estimate for the laser power sufficient for achieving self-focusing.

For sufficient power the ponderomotive force can expel all electrons from the pulse region. They are forced back due to the charge separation, with a blowout region forming behind the pulse [83], which under some conditions can be in the form of an almost spherical bubble [84–86]. The radius, R of such a plasma bubble is dependent on the laser intensity and plasma density and can be estimated as

$$R \approx 2\sqrt{a_0}/k_p \tag{5.5}$$

where k_p the plasma wavelength and the laser spot-size w_0 is matched such that $R \sim w_0$.

The accelerated electrons are not limited in velocity by the pulse which they follow. They are accelerated by the charge separation and once they reach high enough energies, their velocity can exceed that of the plasma wake and the laser pulse (which speed in the plasma is smaller than the speed of light in vacuum). With time, they can thus move from the accelerating fields in the back to the decelerating fields in the front of the plasma wake, and catch up with the pulse. From estimates of the velocities on can deduce the *dephasing length* [85, 86]

$$L_{\mathrm{D}} = \frac{2}{3}\frac{\omega_0^2}{\omega_p^2}R, \tag{5.6}$$

the distance after which the particles catch up with the pulse.

Depending on the plasma density and laser energy and focus, there are different regimes of LWFA. Given a certain laser system one could either i) focus this tightly to get intense fields (large a_0) in a higher density plasma or ii) have a less tight focus (lower a_0) in a lower density plasma. In i),

the high density gives a smaller cavity with large fields accelerating the particles. However, the plasma wave moves with a lower speed and the dephasing length is shorter. In ii), the low density gives a larger cavity with smaller fields for acceleration. However, the plasma wave moves with a higher speed and the dephasing length is longer. E.g. if the aim is to achieve a maximum electron energy, it turns out to be most efficient to pick ii), a lower density plasma and less focused pulse.

Chapter 6

Radiation in laser wakefield acceleration

There are many possible applications of LWFA. The short laser pulses opens up for creating novel X-ray sources [87–90], with short duration, small divergence[62, 63, 91], originating from a μm sized region [92, 93]. Radiation can be generated by oscillations of the electron bunch [94] inside the plasma wave, by collision with a laser pulse [95–100], by collision with a high Z metal or by injection into some external device e.g. a wiggler or undulator [101]. The resultant X-ray bursts can e.g. be used in delicate imaging techniques such as X-ray phase contrast imaging or X-ray absorption spectroscopy [3, 4].

Here we first consider the radiation from two interacting wakefields, considered in Paper V. Finally we, consider the effect of including radiation reaction losses in high intensity LWFA to determine the major effects and for what intensities these are present, considered in Paper VI.

6.1 Radiation emission from interacting wakefields

In Paper V [102], we consider the collision between two laser wakefields with different collision angles. A schematic picture of the setup can be seen in Fig. 6.1, where the wakefields and energetic electron bunches collide at an angle θ, generating X-ray radiation in the process. Radiation is emitted as the electron bunches are accelerated by strong EM fields. In the setup, the origin of these fields depend on the collision angle. For a large angle (e.g. head on) collision, it is the fields from the opposite laser pulse which provides the accelerating fields. On the other hand, when the collisional angle is small (e.g. 10°), the electrons do not interact with the opposite laser pulse as they i) don't spatially overlap and ii) the effective field strength is reduced by the co-propagation. Instead, it is the plasma fields in the combined bubble which provides the accelerating fields. This can be seen in Fig. 6.1 (right panel)

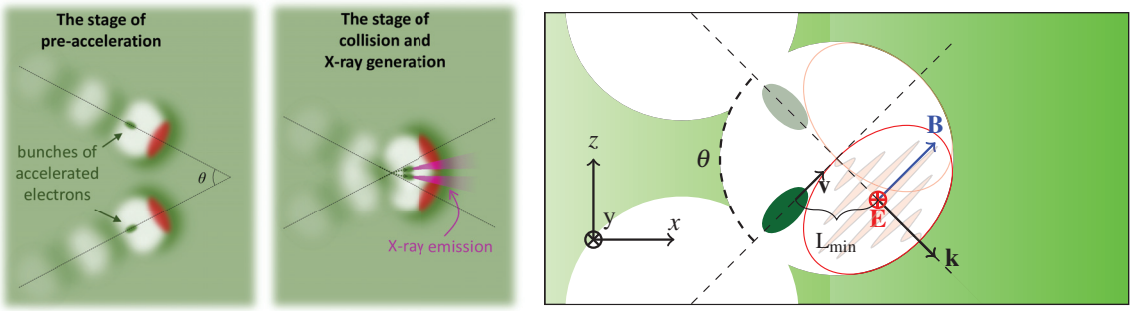

Figure 6.1: From [102]. Schematic pictures of collision setup, showing the collision (left) and the details of pulse and bunch overlap (right).

where one can imagine different values of θ.

The strength of the field can be described by the respective *efficient magnetic field*, see Eq. (4.1), describing the field's ability to provide a transverse acceleration of the particles providing high energy synchrotron emission. For the laser field this depends on the field strength and the collision angle θ and can be estimated as

$$H_{\text{laser}} = A\big(1 - \cos\theta\big) \exp\left[-\cos^2(\theta/2)\right] \ , \tag{6.1}$$

where A is the peak amplitude of the pulse. For the plasma fields the effective magnetic field is given by the plasma density n_0 and the bubble radius R (which in turn is dependent on the laser amplitude) according to

$$H_{\text{plasma}} = \tfrac{4}{3}\pi e n_0 R. \tag{6.2}$$

We perform a number of simulations for different collision angles, keeping track of the emitted radiation. The resultant radiation spectra can be seen in Fig. 6.2, with estimations based on the respective effective field and electron energy estimations. The highest photon frequencies and total energy occur for the high angle, head on collisions. However, also small angle collision provide substantial X-ray radiation.

Furthermore, for small, but still nonzero, angles (5° in our simulations) we observe the merging of wakefields with strong and stable oscillations of the electron bunches, as can be seen in Fig. 6.3. This could substantially increase the interaction time to get a stable and efficient conversion of laser energy to X-ray energy. The angle is small compared to the other considered angles, but still large enough to allow for an experimental setup.

The force on the electron bunch at a distance r from the center is essentially given by the ions inside the sphere of radius r. When the particle is in the center, the force is thus zero and the further from the center the bunch is, the larger the force. The resultant force is that of a harmonic oscillator, and we can calculate an oscillation frequency. Comparing the oscillation period to the typical time of collision, we see that for small collision angles the collision time is longer than the oscillation time, allowing oscillations to form. This is indeed what we see in the simulations.

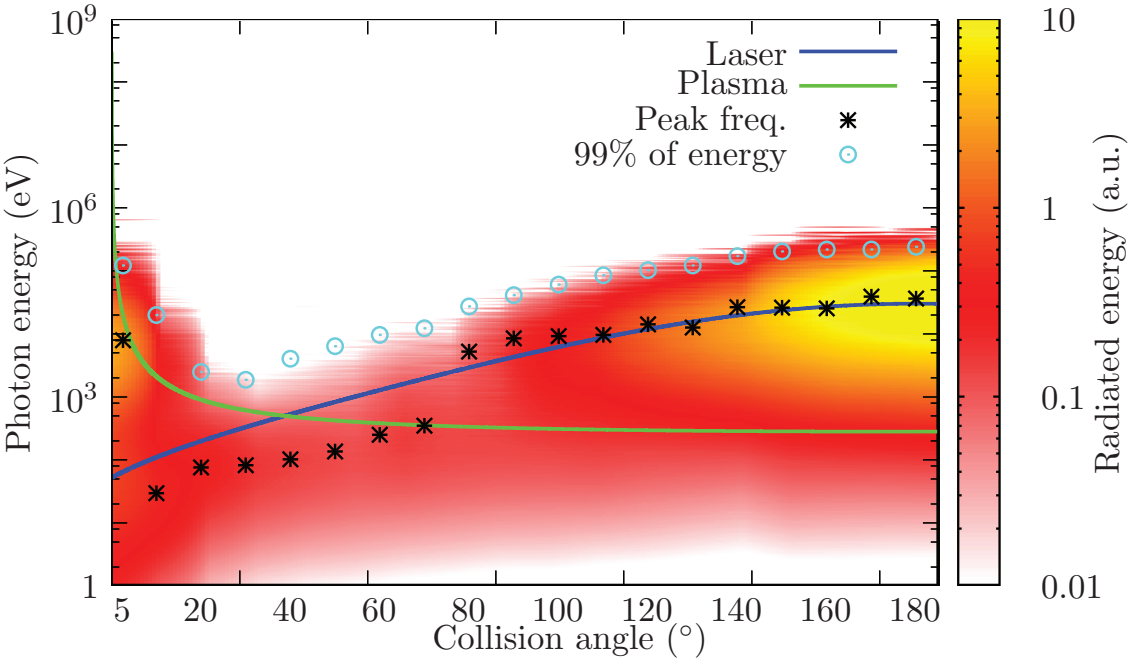

Figure 6.2: From [102]. Emission spectra as a function of collision angle between two laser wakefields. The marks represent the peak frequency and the frequency for below which 99% of the energy is contained. The lines represent estimations of typical emission frequency for the two regimes, based on Eqs. (6.1-6.2), Eq. (3.5) and estimations for the electron energies.

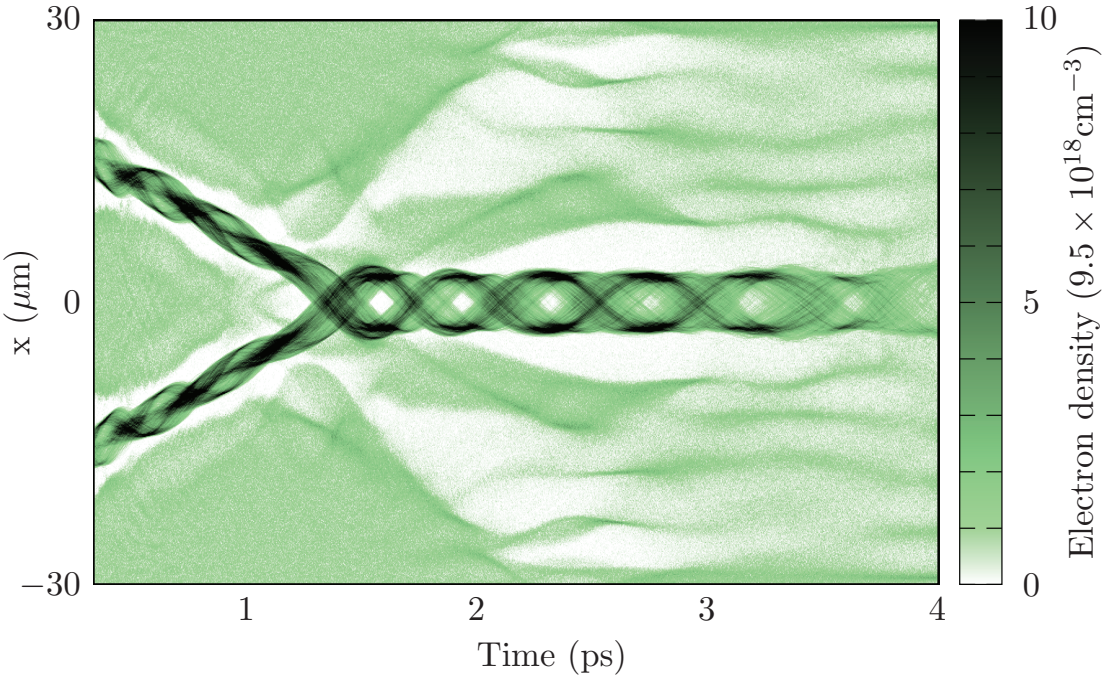

Figure 6.3: From [102]. Cross section of simulation box at bunch position for the duration of the 5° collision simulation, showing oscillatory motion of electron bunches.

6.2 Radiation reaction in LWFA

Much effort in LWFA has been put into achieving as high energy electrons as possible [85, 86, 103], with state-of-the-art laser facilities achieving electrons with energy of GeV [63, 104–107], or even several GeV [12]. As mentioned in Section 5.3, it turns out that the best strategy is not to focus the laser pulse to achieve the most intense fields possible, but to chose a wider focus, less intense fields and a lower plasma density as the longer dephasing length compensates for the smaller accelerating fields. In such attempts, any radiation from the electrons is a parasitic effect as it provides energy loss for the electrons. This is the radiation reaction mentioned previously. Furthermore, the emission of high energy X-rays from the bunch electrons can also be an aim in itself, due to the many applications of short bursts of X-rays.

In Paper VI [108], we consider another regime of LWFA, with intense laser pulses and a close to overdense plasma. We send pulses of different energy and intensity (from $10^{20}\mathrm{W/cm^2}$ to $10^{24}\mathrm{W/cm^2}$) onto the plasma and evaluate the effect of radiation reaction on the result. That is, we consider simulations in which we have modified the classical PIC scheme to include radiation losses, to when radiation reaction is not accounted for. In the latter situation the electrons thus (unphysically) don't lose energy due to radiation. For the intensity of current laser facilities (around $10^{21}\mathrm{W/cm^2}$) this has no significant effect, but for higher intensities in planned facilities this can be of importance.

For cases with and without radiation reaction included and different laser intensities, we measure the evolution of the laser pulse, the particle energies and the emitted radiation. We get information on when radiation reaction is of importance in LWFA, for e.g. the energy of the bunch electrons and the energy depletion of the pulse. Some results can be seen in Figs. 6.4 and 6.5. Fig. 6.4 shows ratios for electron energy (red, left side) and pulse depletion distance (blue, right side), between cases without radiation reaction and with radiation reaction included, for different intensities. For intensities from $10^{22}\mathrm{W/cm^2}$ the electron energy starts to be affected and for intensities above 10^{23} $\mathrm{W/cm^2}$ the pulse propagation distance is affected by the radiation loss.

In Fig. 6.5 we consider the conversion of field (laser) energy into electron energy, ion energy and high frequency radiation respectfully, here shown for the case of laser intensity $4 \times 10^{24}\mathrm{W/cm^2}$ with and without the inclusion of radiation reaction. In this regime of LWFA, a large part of the initial laser pulse energy is converted into high frequency X-ray radiation.

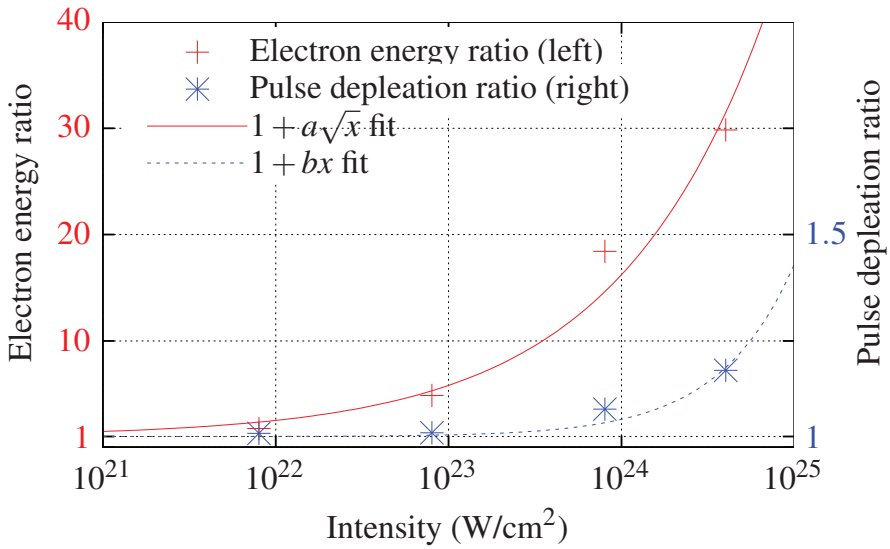

Figure 6.4: From [108]. Ratio of maximum electron energies (red, left) without and with RR included and ratio of pulse depletion distances (blue/dashed, right) without and with radiation reaction included.

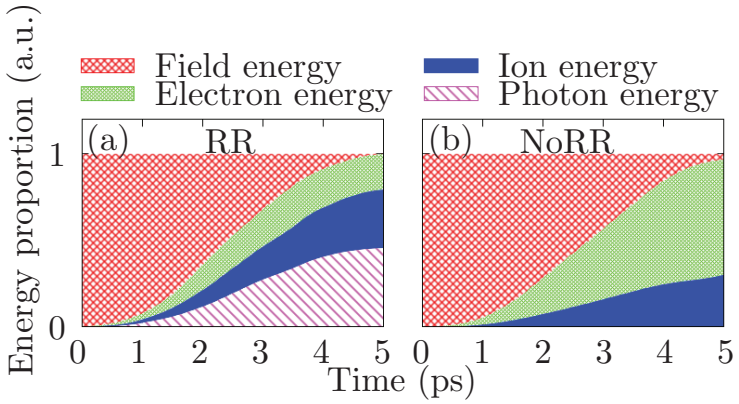

Figure 6.5: From [108]. Energy partitioning as a function of time, for the case of laser intensity $4 \times 10^{24}\mathrm{W/cm^2}$. Energy is redistributed from laser pulse energy to electrons, ions and photons. When radiation reaction is not properly modelled the electrons don't lose energy through radiation and their energy is overestimated.

Chapter 7

Summary of papers

Paper 1

Three-wave interaction and Manley-Rowe relations in quantum hydrodynamics

In this paper we show that the equations for quantum hydrodynamics with a generalized Bohm de Broglie force fulfil the Manley-Rowe relations only for the standard form of the Bohm de Broglie force. This adds further weight to the standard expression for the Bohm de Broglie term, whose derivation to some extent lacks a firm base.

My contribution to this paper was to perform the calculations of the coupled three-wave interaction to show the main result of how the Manley-Rowe relations where fulfilled. I also contributed to deriving the coupled equations for the amplitudes and to writing the paper.

Paper 2

Narrowing of the emission angle in high-intensity Compton scattering

In this paper we implement the calculation of the classical radiation spectra from relativistic particles, in the one-particle code *Simla* [44]. This simulates the collision of a particle with a realistic laser pulse and is capable of using different equations of motion, including a stochastic QED one. We compare the radiation spectra between runs using a classical equation of motion and runs using a QED equation.

My contribution to this paper was to implement the numerical method for the emission of classical radiation into the single-particle code and contributing to writing a part of the paper.

Paper 3

Effects of high energy photon emissions in laser generated ultra-relativistic plasmas: Real-time synchrotron simulations

In this paper we develop a runtime numerical Monte Carlo method for the calculation of the radiation emission spectra for relativistic particles in simulations. We test the method by comparing the emitted energy to the energy loss due to radiation reaction, calculated using the L.L. method, in a particle-in-cell laser wakefield acceleration simulation. The simulations show excellent agreement between the two methods. *My contribution to this paper was to develop and implement the numerical method, run the simulations and to writing the paper*

Paper 4

Extended particle-in-cell schemes for physics in ultra-strong laser fields: Review and developments In this paper we review common extensions of the particle-in-cell scheme in order to permit simulations of plasmas interacting with high intensity lasers. Furthermore, we propose a number of new solutions regarding these techniques.

My contribution to this paper was to be part of the development and implementation of the PIC extensions, in particular regarding the emission of classical synchrotron radiation. I also contributed to the writing of the part of the dual treatment of the electromagnetic field.

Paper 5

Radiation emission from braided electrons in interacting wakefields In this paper we propose a novel method for generation of electromagnetic radiation from laser wakefield acceleration, by the means of colliding two wakefields at different angles. We perform 3D particle-in-cell simulations to show that there are two regimes where, depending on the collision angle, the EM radiation from the electron bunches is due either to acceleration from the plasma field or the laser field. Furthermore, we demonstrate that the wakefields can merge to form a new structure with the motion of the electron bunches forming a braided pattern, with the potential of providing a stable conversion of laser energy to X-ray energy.

My contribution to this paper was performing all the simulations and data analysis, make theoretical estimations and to the writing of the paper.

Paper 6

Propagation of Ultra-Intense Laser Pulses in Near-critical Plasmas: Depletion Mechanisms and Effects of Radiation Reaction

In this paper we do a number of laser wakefield acceleration simulations, where we increase the energy of the laser shot at the plasma. For the higher energy cases the laser intensity, and the subsequent particle energy, is high enough for radiation reaction to affect the dynamics of the particles. We investigate the effect of this and how the laser energy is transformed into particle- and radiation energy.

My contribution to this paper was performing all the simulations and data analysis and to the writing of the paper.

Acknowledgments

There are many people I would like to thank. Firstly my supervisors, Mattias and Gert. Thanks for hiring me, for believing in me and for the practical solution of working 1000 km away. Collaboration over distance is not the most easy or efficient method but I'm happy we worked it out. Here I would like to thank Arkady for always being available for invaluable support in numerical methods and for excellent interpretation of uncommented code!

I would also like to thank all past and present group members. Without you I could have spent twice as much time on research, but I would only have had half the fun! Special mention to Jens, Martin, Mats, Joakim, Chris, Arkady, Anton, Greger, Amol, Robin, Joel, Tom and Benjamin. It's been great to work with you!

To all the administrative personnel in Umeå, Thank you! To all the administrative personnel in Gothenburg, I'm sorry! It's natural to connect with those you meet every day, and tasks might be prioritised thereafter. I'm sorry for all reminders, I'm happy for all support to my unofficial distance PhD. Special Umeå mentions to Jörgen, Ann-Charlott and Katarina and thanks to everybody else I've met in the covfeferoom through the years.

I would also like to thank all great developers of open-source software. This thesis was typeset in LaTeX, with figures in PGFTi*k*Z, PGFPlots and gnuplot, written in emacs on an archlinux distribution, with many more great applications used in the research. Even thank you to all developers of console email clients, though the mere thought will cost me another two days.

Finally, I would like to thank family and friends for support, amusement and distraction. Especially my wife Elin, without which this thesis might not have been written, and our children Emil and Agnes, without which this thesis would have been written years ago.

Bibliography

[1] C. Chiu, M. Fomytskyi, F. Grigsby, F. Raischel, M. C. Downer, and T. Tajima. Laser electron accelerators for radiation medicine: a feasibility study. *Medical physics*, 31(7):2042–2052, 2004.

[2] S.V. Bulanov and V.S. Khoroshkov. Feasibility of using laser ion accelerators in proton therapy. *Plasma Physics Reports*, 28(5):453–456, 2002.

[3] F. Albert, A.G.R. Thomas, S.P.D. Mangles, S. Banerjee, S. Corde, A. Flacco, M. Litos, D. Neely, J. Vieira, Z. Najmudin, et al. Laser wakefield accelerator based light sources: potential applications and requirements. *Plasma Physics and Controlled Fusion*, 56(8):084015, 2014.

[4] F. Albert and A. G.R. Thomas. Applications of laser wakefield accelerator-based light sources. *Plasma Physics and Controlled Fusion*, 58(10):103001, 2016.

[5] L. Evans and P. Bryant. Lhc machine. *Journal of instrumentation*, 3(08):S08001, 2008.

[6] SLAC: https://www6.slac.stanford.edu/.

[7] W. Leemans, P. Catravas, E. Esarey, C. Geddes, C. Toth, R. Trines, C. Schroeder, B. Shadwick, J. van Tilborg, and J. Faure. Electron-Yield Enhancement in a Laser-Wakefield Accelerator Driven by Asymmetric Laser Pulses. *Phys. Rev. Lett.*, 89(17):174802, October 2002.

[8] V. Malka, S. Fritzler, E. Lefebvre, and M.M. Aleonard. Electron acceleration by a wake field forced by an intense ultrashort laser pulse. *Science*, 298(November):1596–1601, 2002.

[9] A. Modena, Z. Najmudin, A. Dangor, E., C. E. Clayton, K. A. Marsh, C. Joshi, V. Malka, C. B. Darrow, C. Danson, D. Neely, and F. N. Walsh. Electron acceleration from the breaking of relativistic plasma waves. *Nature*, 377, 1995.

[10] S. M. Hooker. Developments in laser-driven plasma accelerators. *Nature Photonics*, 7(10):775, 2013.

[11] E Esarey. E. esarey, cb schroeder, and wp leemans, rev. mod. phys. 81, 1229 (2009). *Rev. Mod. Phys.*, 81:1229, 2009.

[12] W.P. Leemans, A.J. Gonsalves, H.S. Mao, K. Nakamura, C. Benedetti, C.B. Schroeder, C. Tóth, J. Daniels, D.E. Mittelberger, S.S. Bulanov, et al. Multi-gev electron beams from capillary-discharge-guided subpetawatt laser pulses in the self-trapping regime. *Phys. Rev. Lett.*, 113(24):245002, 2014.

[13] D. Strickland and G. Mourou. Compression of amplified chirped optical pulses. *Opt. Comm.*, 56(3):219–221, 1985.

[14] V. Yanovsky, V. Chvykov, G. Kalinchenko, P. Rousseau, T. Planchon, T. Matsuoka, A. Maksimchuk, J. Nees, G. Cheriaux, G. Mourou, et al. Ultra-high intensity-300-TW laser at 0.1 hz repetition rate. *Opt. Express*, 16(3):2109–2114, 2008.

[15] M. Roth, A. Blazevic, M. Geissel, T. Schlegel, T.E. Cowan, M. Allen, J.-C. Gauthier, P. Audebert, J. Fuchs, J. Meyer-ter Vehn, et al. Energetic ions generated by laser pulses: A detailed study on target properties. *Physical Review Special Topics-Accelerators and Beams*, 5(6):061301, 2002.

[16] P. Mora. Plasma expansion into a vacuum. *Physical Review Letters*, 90(18):185002, 2003.

[17] M. Passoni, L. Bertagna, and A. Zani. Target normal sheath acceleration: theory, comparison with experiments and future perspectives. *New Journal of Physics*, 12(4):045012, 2010.

[18] I.C.E. Turcu, C. Murphy, F. Negoita, D. Stutman, M. Zepf, J. Schreiber, C. Harvey, R.J. Gray, M. Toma, S. Balascuta, et al. High field physics and qed experiments at eli-np. *Rom. Rep. Phys.*, 68:S145, 2016.

[19] J.M. Dawson. Particle simulation of plasmas. *Rev.Mod. Phys.*, 1983.

[20] C.K. Birdsall and A.B. Langdon. Plasma physics via computer simulation. 1985.

[21] L. Tonks and I. Langmuir. Oscillations in ionized gases. *Phys. Rev.*, 33(2):195, 1929.

[22] P. Debye and E. Hyckel. De la théorie des électrolytes. i. abaissement du point de congélation et phénomènes associés. *Phys. Zeitz.*, 24(9):185–206, 1923.

[23] D.R. Nicholson. *Introduction to plasma theory*. Cambridge Univ Press, 1983.

[24] A. A. Vlasov. *J. Phys. U.S.S.R.*, 9(25), 1945.

[25] L.D. Landau. On the vibrations of the electronic plasma. *J. Phys. U.S.S.R.*, 10(25), 1946.

[26] J.M. Manley and H.E. Rowe. Some general properties of nonlinear elements-part i. general energy relations. *Proceedings of the IRE*, 44(7):904–913, 1956.

[27] J. Larsson. A new Hamiltonian formulation for fluids and plasmas. part 3. Multifluid electrodynamics. *J. Plasma Phys.*, 55:279–300, 4 1996.

[28] I.Y. Dodin, A.I. Zhmoginov, and N.J. Fisch. Manley–Rowe relations for an arbitrary discrete system. *Physics Letters A*, 372(39):6094–6096, 2008.

[29] E. Wallin, J. Zamanian, and G. Brodin. Three-wave interaction and Manley–Rowe relations in quantum hydrodynamics. *J. Plasma Phys.*, 80(04):643–652, 2014.

[30] J. Lundin, J. Zamanian, M. Marklund, and G. Brodin. Short wavelength electromagnetic propagation in magnetized quantum plasmas. *Phys. Plasmas*, 14:062112, 2007.

[31] F. Haas. *Quantum Plasmas*. Springer, New York, 2011.

[32] G. Manfredi. How to model quantum plasmas. In C. Sulem T. Passot and P.-L. Sulem, editors, *Topics in Kinetic Theory*. Fields Institute Communications, 2005.

[33] G. Manfredi and F. Haas. Self-consistent fluid model for a quantum electron gas. *Phys. Rev. B*, 64(7):075316, 2001.

[34] D. A. Burton and A. Noble. Aspects of electromagnetic radiation reaction in strong fields. *Contemporary Physics*, 55(2):110–121, 2014.

[35] M. Vranic, J. L. Martins, R. A. Fonseca, and L. O. Silva. Classical radiation reaction in particle-in-cell simulations. *Computer Physics Communications*, 204:141–151, 2016.

[36] A. Ilderton and G. Torgrimsson. Radiation reaction from QED: light-front perturbation theory in a plane wave background. *Phys.Rev.*, D88(2):025021, 2013.

[37] J.M. Cole, K.T. Behm, E. Gerstmayr, T.G. Blackburn, J.C. Wood, C.D. Baird, M.J. Duff, C. Harvey, A. Ilderton, A.S. Joglekar, et al. Experimental evidence of radiation reaction in the collision of a high-intensity laser pulse with a laser-wakefield accelerated electron beam. *Physical Review X*, 8(1):011020, 2018.

[38] K. Poder, M. Tamburini, G. Sarri, A. Di Piazza, S. Kuschel, C.D. Baird, K. Behm, S. Bohlen, J.M. Cole, M. Duff, et al. Evidence of strong radiation reaction in the field of an ultra-intense laser. *arXiv preprint arXiv:1709.01861*, 2017.

[39] J.D. Jackson. Classical electrodynamics. *Classical Electrodynamics, 3rd Edition, by John David Jackson, pp. 832. ISBN 0-471-30932-X. Wiley-VCH, July 1998.*, 1, 1998.

[40] L.D. Landau and E.M. Lifshitz. The classical theory of fields. *Elsevier, Oxford*, 1975.

[41] V.B. Berestretski, E.M. Lifshitz, and L.P. Pitaevskii. Quantum electrodynamics (course of theoretical physics, ser. vol. 4), 1982.

[42] C. N. Harvey, A. Gonoskov, M. Marklund, and E. Wallin. Narrowing of the emission angle in high-intensity compton scattering. *Phys. Rev. A*, 93:022112, Feb 2016.

[43] A. Gonoskov, S. Bastrakov, E. Efimenko, A. Ilderton, M. Marklund, I. Meyerov, A. Muraviev, A. Sergeev, I. Surmin, and E. Wallin. Extended particle-in-cell schemes for physics in ultrastrong laser fields: Review and developments. *Phys. Rev. E*, 92:023305, Aug 2015.

[44] D.G. Green and C.N. Harvey. Simla: Simulating particle dynamics in intense laser and other electromagnetic fields via classical and quantum electrodynamics. *Computer Physics Communications*, 192:313–321, 2015.

[45] C. Harvey, T. Heinzl, and A. Ilderton. Signatures of high-intensity compton scattering. *Phys. Rev. A*, 79:063407, Jun 2009.

[46] K.S. Yee et al. Numerical solution of initial boundary value problems involving maxwell's equations in isotropic media. *IEEE Trans. Antennas Propag*, 14(3):302–307, 1966.

[47] B. Gustafsson, H.O. Kreiss, and J. Oliger. *Time dependent problems and difference methods*, volume 24. John Wiley & Sons, 1995.

[48] J.P. Boris. Relativistic plasma simulation-optimization of a hybrid code. In *Proc. Fourth Conf. Num. Sim. Plasmas, Naval Res. Lab, Wash. DC*, pages 3–67, 1970.

[49] F. Peano, M. Marti, L. O. Silva, and G. Coppa. Statistical kinetic treatment of relativistic binary collisions. *Phys. Rev. E*, 79:025701, Feb 2009.

[50] M. Chen, E. Cormier-Michel, C.G.R. Geddes, D.L. Bruhwiler, L.L. Yu, E. Esarey, C.B. Schroeder, and W.P. Leemans. Numerical modeling of laser tunneling ionization in explicit particle-in-cell codes. *J Comput. Phys.*, 236:220–228, 2013.

[51] ELI: www.extreme-light infrastructure.eu.

[52] XCELS: www.xcels.iapras.ru.

[53] Vulcan: www.clf.stfc.ac.uk.

[54] M. Tamburini, F. Pegoraro, A. Di Piazza, C.H. Keitel, and A. Macchi. Radiation reaction effects on radiation pressure acceleration. *New J. Phys.*, 12(12):123005, 2010.

[55] M. Chen, A. Pukhov, T.-P. Yu, and Z.-M. Sheng. Radiation reaction effects on ion acceleration in laser foil interaction. *Plasma Physics and Controlled Fusion*, 53(1):014004, 2010.

[56] R. Bach, D. Pope, S.-H. Liou, and H. Batelaan. Controlled double-slit electron diffraction. *New Journal of Physics*, 15(3):033018, 2013.

[57] E. Wallin, A. Gonoskov, and M. Marklund. Effects of high energy photon emissions in laser generated ultra-relativistic plasmas: real-time synchrotron simulations. *Phys. Plasmas*, 22:033117, 2015.

[58] A. Gonoskov. Ultra-intense laser-plasma interaction for applied and fundamental physics. *Ph.D. thesis, Umea University*, 2013.

[59] A. Pukhov and J. Meyer-ter Vehn. Laser wake field acceleration: the highly non-linear broken-wave regime. *Appl. Phys. B*, 74(4-5):355–361, 2002.

[60] T. Tajima and J.M. Dawson. Laser electron accelerator. *Phys. Rev. Lett.*, 43(4):267–270, 1979.

[61] P. Sprangle, E. Esarey, a. Ting, and G. Joyce. Laser wakefield acceleration and relativistic optical guiding. *Appl. Phys. Lett.*, 53(22):2146, 1988.

[62] C.G.R. Geddes, C. Toth, and J. Van Tilborg. High-quality electron beams from a laser wakefield accelerator using plasma-channel guiding. *Nature*, 431(September), 2004.

[63] W.P. Leemans, B. Nagler, A.J. Gonsalves, C. Toth, K. Nakamura, C.G.R. Geddes, E. Esarey, C.B. Schroeder, and S.M. Hooker. GeV electron beams from a centimetre-scale accelerator. *Nature Phys.*, 2(10):696–699, 2006.

[64] S. Corde, K. Ta Phuoc, G. Lambert, R. Fitour, V. Malka, A. Rousse, A. Beck, and E. Lefebvre. Femtosecond x-rays from laser-plasma accelerators. *Rev. Mod. Phys.*, 85(1):1–48, 2013.

[65] A. Rousse, K.T. Phuoc, R. Shah, and A. Pukhov. Production of a kev x-ray beam from synchrotron radiation in relativistic laser-plasma interaction. *Phys. Rev. Lett.*, 93(13):135005, Sep 2004.

[66] E. N. Nerush, I. Y. Kostyukov, A. M. Fedotov, N. B. Narozhny, N. V. Elkina, and H. Ruhl. Laser field absorption in self-generated electron-positron pair plasma. *Phys. Rev. Lett.*, 106:035001, Jan 2011.

[67] N. V. Elkina, A. M. Fedotov, I. Y. Kostyukov, M. V. Legkov, N. B. Narozhny, E. N. Nerush, and H. Ruhl. Qed cascades induced by circularly polarized laser fields. *Phys. Rev. ST Accel. Beams*, 14:054401, May 2011.

[68] I. V. Sokolov, N. M. Naumova, and J. A. Nees. Numerical modeling of radiation-dominated and quantum-electrodynamically strong regimes of laser-plasma interaction. *Physics of Plasmas*, 18(9):–, 2011.

[69] C.P. Ridgers, J.G. Kirk, R. Duclous, T.G. Blackburn, C.S. Brady, K. Bennett, T.D. Arber, and A.R. Bell. Modelling gamma-ray photon emission and pair production in high-intensity laser–matter interactions. *Journal of Computational Physics*, 260(0):273 – 285, 2014.

[70] H. Lehmann, K. Symanzik, and W. Zimmermann. On the formulation of quantized field theories. II. *Nuovo Cim.*, 6:319–333, 1957.

[71] H. Lehmann, K. Symanzik, and W. Zimmermann. On the formulation of quantized field theories. *Nuovo Cim.*, 1:205–225, 1955.

[72] A. I. Nikishov and V. I. Ritus. Quantum processes in the field of a plane electromagnetic wave and in a constant field, 1. *Sov. Phys. JETP*, 19:529, 1964.

[73] A. I. Nikishov and V. I. Ritus. Pair production by a photon and photon emission by an electron in the field of an intense electromagnetic wave and in a constant field. *Sov. Phys. JETP*, 25:1135, 1967.

[74] A. I. Nikishov and V. I. Ritus. Quantum processes in the field of a plane electromagnetic wave and in a constant field. *Sov. Phys. JETP*, 19:1191, 1964.

[75] A. Higuchi and G.D.R. Martin. Radiation reaction on charged particles in three-dimensional motion in classical and quantum electrodynamics. *Phys.Rev.*, D73:025019, 2006.

[76] A. Di Piazza, K.Z. Hatsagortsyan, and C.H. Keitel. Quantum radiation reaction effects in multiphoton Compton scattering. *Phys.Rev.Lett.*, 105:220403, 2010.

[77] A. Di Piazza, C. Muller, K.Z. Hatsagortsyan, and C.H. Keitel. Extremely high-intensity laser interactions with fundamental quantum systems. *Rev.Mod.Phys.*, 84:1177, 2012.

[78] A. Ilderton and G. Torgrimsson. Radiation reaction in strong field QED. *Phys. Lett. B*, 725:481, 2013.

[79] V.S. Krivitsky and V.N. Tsytovich. Average radiation reaction force in quantum electrodynamics. *Sov.Phys.Usp.*, 34:250–258, 1991.

[80] A.I. Voroshilo, E.A. Padusenko, and S.P. Roshchupkin. One-photon annihilation of an electron-positron pair in the field of pulsed circularly polarized light wave. *Laser physics*, 20(7):1679–1685, 2010.

[81] A. Ilderton. Trident pair production in strong laser pulses. *Phys.Rev.Lett.*, 106:020404, 2011.

[82] B. King and H. Ruhl. Trident pair production in a constant crossed field. *Phys.Rev.*, D88(1):013005, 2013.

[83] G.-Z. Sun, E. Ott, Y.C. Lee, and P. Guzdar. Self-focusing of short intense pulses in plasmas. *The Physics of fluids*, 30(2):526–532, 1987.

[84] I. Kostyukov, A. Pukhov, and S. Kiselev. Phenomenological theory of laser-plasma interaction in "bubble" regime. *Physics of Plasmas*, 11(11):5256–5264, 2004.

[85] W. Lu, C. Huang, M. Zhou, W.B. Mori, and T. Katsouleas. Nonlinear theory for relativistic plasma wakefields in the blowout regime. *Phys. Rev. Lett.*, 96(16):165002, 2006.

[86] W. Lu, C. Huang, M. Zhou, M. Tzoufras, F.S. Tsung, W.B. Mori, and T. Katsouleas. A nonlinear theory for multidimensional relativistic plasma wave wakefieldsa). *Phys. Plasmas*, 13(5):056709, 2006.

[87] E. Esarey, B. A. Shadwick, P. Catravas, and W. P. Leemans. Synchrotron radiation from electron beams in plasma-focusing channels. *Phys. Rev. E*, 65:056505, May 2002.

[88] K. Németh, B. Shen, Y. Li, H. Shang, R. Crowell, K. C. Harkay, and J. R. Cary. Laser-driven coherent betatron oscillation in a laser-wakefield cavity. *Phys. Rev. Lett.*, 100:095002, Mar 2008.

[89] A. Rousse, K. T. Phuoc, R. Shah, A. Pukhov, E. Lefebvre, V. Malka, S. Kiselev, F. Burgy, J.-P Rousseau, D. Umstadter, and D. Hulin. Production of a kev x-ray beam from synchrotron radiation in relativistic laser-plasma interaction. *Phys. Rev. Lett.*, 93:135005, Sep 2004.

[90] S. Cipiccia, M. R. Islam, B. Ersfeld, R. P. Shanks, E. Brunetti, G. Vieux, X. Yang, R. C. Issac, S. M. Wiggins, G. H. Welsh, M.-P. Anania, D. Maneuski, R. Montgomery, G. Smith, M. Hoek, D. J. Hamilton, N. R. C. Lemos, D. Symes, P. P. Rajeev, V. O. Shea, J. M. Dias, and D. A. Jaroszynski. Gamma-rays from harmonically resonant betatron oscillations in a plasma wake. *Nature Physics*, 7:867–871, November 2011.

[91] K. T. Phuoc, S. Corde, R. Shah, F. Albert, R. Fitour, J.-P. Rousseau, F. Burgy, B. Mercier, and A. Rousse. Imaging electron trajectories in a laser-wakefield cavity using betatron x-ray radiation. *Physical review letters*, 97(22):225002, 2006.

[92] S. Kneip, C. McGuffey, J.L. Martins, S.F. Martins, C. Bellei, V. Chvykov, F. Dollar, R. Fonseca, C. Huntington, G. Kalintchenko, et al. Bright spatially coherent synchrotron x-rays from a table-top source. *Nature Physics*, 6(12):980, 2010.

[93] R. C. Shah, F. Albert, K. Ta. Phuoc, O. Shevchenko, D. Boschetto, A. Pukhov, S. Kiselev, F. Burgy, J.-P. Rousseau, and A. Rousse. Coherence-based transverse measurement of synchrotron x-ray radiation from relativistic laser-plasma interaction and laser-accelerated electrons. *Physical Review E*, 74(4):045401, 2006.

[94] S. Kiselev, A. Pukhov, and I. Kostyukov. X-ray Generation in Strongly Nonlinear Plasma Waves. *Phys. Rev. Lett.*, 93(13):135004, September 2004.

[95] P. Sprangle, A. Ting, E. Esarey, and A. Fisher. Tunable, short pulse hard x-rays from a compact laser synchrotron source. *J. Appl. Phys.*, 72(11):5032–5038, 1992.

[96] P. Catravas, E. Esarey, and W. P. Leemans. Femtosecond x-rays from Thomson scattering using laser wakefield accelerators. *Meas. Sci. Technol.*, 12(11):1828–1834, 2001.

[97] H. Schwoerer, B. Liesfeld, H. P. Schlenvoigt, K. U. Amthor, and R. Sauerbrey. Thomson-backscattered X rays from laser-accelerated electrons. *Phys. Rev. Lett.*, 96(1):1–4, 2006.

[98] K. Ta Phuoc, S. Corde, C. Thaury, V. Malka, A. Tafzi, J. P. Goddet, R. C. Shah, S. Sebban, and A. Rousse. All-optical Compton gamma-ray source. *Nat. Photonics*, 6(5):308–311, 2012.

[99] A. V. Korzhimanov, A. A. Gonoskov, E. A. Khazanov, and A. M. Sergeev. Horizons of petawatt laser technology. *Physics-Uspekhi*, 54(1):9–28, 2011.

[100] H.-E. Tsai, X. Wang, J.M. Shaw, Z. Li, A.V. Arefiev, X. Zhang, R. Zgadzaj, W. Henderson, V. Khudik, G. Shvets, et al. Compact tunable Compton x-ray source from laser-plasma accelerator and plasma mirror. *Physics of Plasmas*, 22(2):023106, 2015.

[101] J. A. Clarke. *The science and technology of undulators and wigglers*. Number 4. Oxford University Press on Demand, 2004.

[102] E. Wallin, A. Gonoskov, and M. Marklund. Radiation emission from braided electrons in interacting wakefields. *Physics of Plasmas*, 24(9):093101, 2017.

[103] W. Lu, M. Tzoufras, C. Joshi, F.S. Tsung, W.B. Mori, J. Vieira, R.A. Fonseca, and L.O. Silva. Generating multi-GeV electron bunches using single stage laser wakefield acceleration in a 3D nonlinear regime. *Phys. Rev. ST Accel. Beams*, 10(6):061301, 2007.

[104] Nasr A.M. Hafz, T.M. Jeong, I.W. Choi, S.K. Lee, K.H. Pae, V.V. Kulagin, J.H Sung, T.J. Yu, K.-H. Hong, T. Hosokai, et al. Stable generation of GeV-class electron beams from self-guided laser–plasma channels. *Nature Photonics*, 2(9):571, 2008.

[105] C.E. Clayton, J.E. Ralph, F. Albert, R.A. Fonseca, S.H. Glenzer, C. Joshi, W. Lu, K.A. Marsh, S.F. Martins, W.B. Mori, et al. Self-guided laser wakefield acceleration beyond 1 GeV using ionization-induced injection. *Physical review letters*, 105(10):105003, 2010.

[106] H.T. Kim, K.H. Pae, H.J. Cha, I.J. Kim, T.J. Yu, J.H. Sung, S.K. Lee, T. M. Jeong, and J. Lee. Enhancement of electron energy to the multi-GeV regime by a dual-stage laser-wakefield accelerator pumped by petawatt laser pulses. *Physical review letters*, 111(16):165002, 2013.

[107] X. Wang, R. Zgadzaj, N. Fazel, Z. Li, S.A Yi, X. Zhang, W. Henderson, Y.-Y. Chang, R. Korzekwa, H.-E. Tsai, et al. Quasi-monoenergetic laser-plasma acceleration of electrons to 2 GeV. *Nature communications*, 4:1988, 2013.

[108] E. Wallin, A. Gonoskov, C. Harvey, O. Lundh, and M. Marklund. Ultra-intense laser pulses in near-critical underdense plasmas–

radiation reaction and energy partitioning. *Journal of Plasma Physics*, 83(2), 2017.